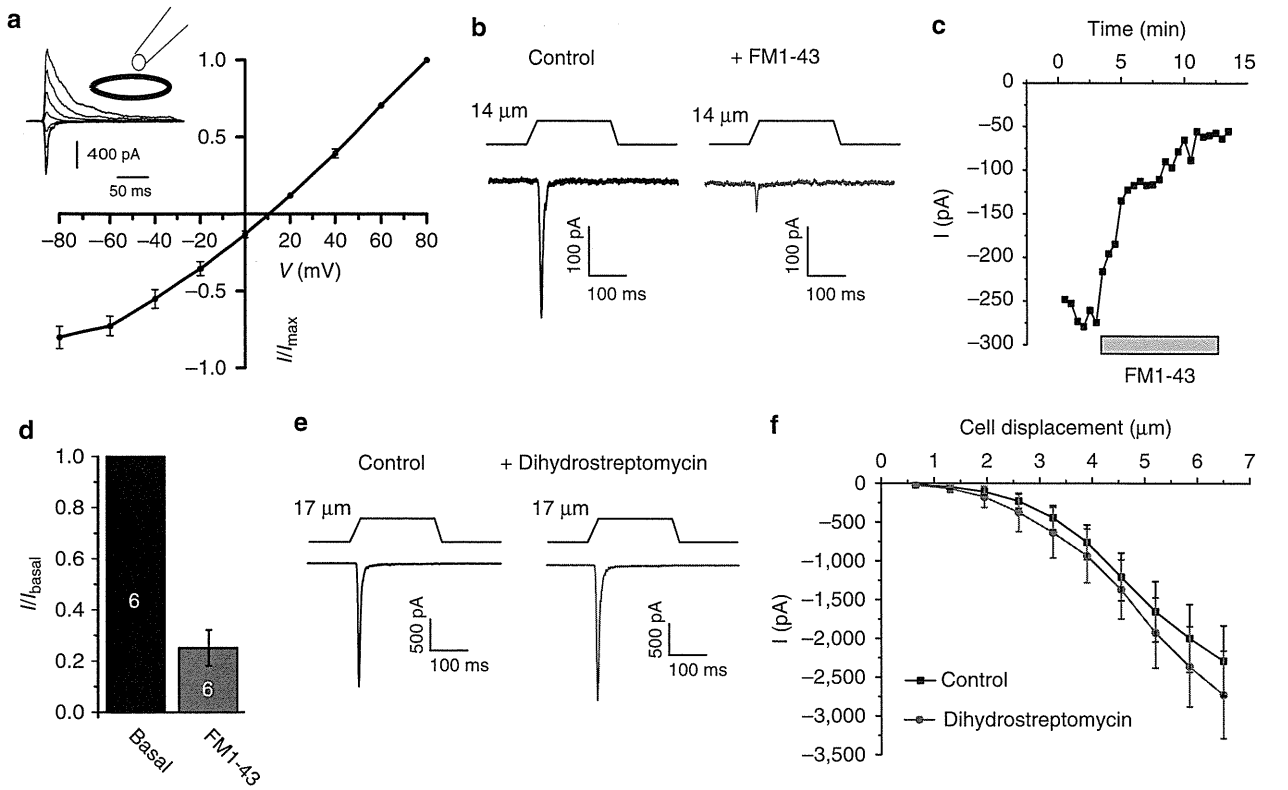

Figure 3 | Biophysical characterization of hPiezo2. (**a**) Mean current voltage relationship of hPiezo2 expressed in HEK293 cells in response to a 4 µm displacements of the membrane ($n=7$). hPiezo2 currents were recorded using the perforated configuration of the whole-cell patch clamp technique. Inset shows example current trace at the different holding voltages. (**b**) Typical steady-state current traces at a holding potential of −70 mV recorded before (control) and after addition of FM1-43 (15 µM) to the bathing solution. Mechanical probe displacement is shown inset (positioned 11 µm from cell). (**c**) Example time course of FM1-43 inhibition showing peak mechanically evoked current in response to a 3-µm membrane displacement. Time at which FM1-43 was added to the bathing solution is indicated by the grey bar. (**d**) Mean fractional inhibition of hPiezo2 currents. Number of experiments is indicated within bars. (**e**) Typical current traces in response to a 6-µm membrane displacement after 15 min preincubation in vehicle (control) or dihydrostreptomycin (10 µM). Mechanical probe displacement is shown inset (positioned 11 µm from cell). (**f**) Mean peak mechanically evoked currents. Data are expressed as mean ± s.e.m.

(Fig. 5a). Importantly, however, 8-pCPT-induced mechanical hypersensitivity lasted significantly longer than 6-Bnz-cAMP-induced mechanical hypersensitivity (Fig. 5b,c). At the highest dose tested (12.5 nmol per paw), 8-pCPT-induced sensitization lasted ~3 days while 6-Bnz-cAMP-induced mechanical hypersensitivity only lasted ~1 day (Fig. 5c).

8-pCPT-induced mechanical sensitization was dependent on DRG Epac1 as intrathecal Epac1 antisense oligodeoxynucleotides (ODNs) administration reduced DRG protein levels for Epac1 by ~44% and almost completely prevented development of mechanical sensitization induced by 8-pCPT (Fig. 5d,e). Epac1 antisense ODN treatment did not affect baseline thresholds to von Frey filaments (Fig. 5e). The Epac1 antisense ODN strategy was confirmed by using Epac1 knockout mice. 8-pCPT-induced mechanical allodynia was prevented in *Epac1*−/− mice (Fig. 5f; $P<0.001$; $n=8$–12; two-way analysis of variance) and *Epac1*+/− mice (Fig. 5f; $P<0.05$; $n=8$–12; two-way analysis of variance). *Epac*+/− mice did not statistically differ from *Epac1*−/− mice. 6-Bnz-cAMP-induced mechanical hypersensitivity was indistinguishable between WT, *Epac1*−/− and *Epac1*+/− mice (Fig. 5g). Thus, the activation of cAMP-sensor Epac1 leads to sensitization that is longer in duration (3–4 days) than PKA-mediated hypersensitivity (<1 day). Importantly, Epac1 antisense-treated and genetically modified mice with low Epac1 protein levels indicate that partial reduction of Epac1 induces large behavioural effects.

To determine whether sensitization of mechanotransducing channels underlies 8-pCPT-induced mechanical allodynia, we used intraplantar FM1-43 that blocks mechanically activated currents in sensory neurons and Piezo2 currents (Fig. 3d)[20]. Intraplantar FM1-43 almost completely reversed 8-pCPT-induced allodynia (Fig. 5h). As shown before[20], injection of FM1-43 doubled the threshold to mechanical stimulation in naive control mice (Fig. 5h). Thus, Epac1 activation causes a long-lasting increase in sensitivity to touch that is mediated through mechanosensitive channels *in vivo*.

Epac signalling enhances wide dynamic range responses to mechanical stimuli. Lamina V wide dynamic range (WDR) neurons in the dorsal horn respond to all sensory modalities. Extracellular recording from rat WDR neurons in response to mechanical input to the receptive field showed that 8-pCPT enhanced WDR neuron firing in response to mechanical stimuli applied to the hind paw that was ≤26 g (Fig. 6a). In contrast, 6-Bnz-cAMP only enhanced WDR neuron firing in response to mechanical stimuli applied to the receptive field (hind paw) that were larger than 15 g (Fig. 6b). Intraplantar injection of saline did

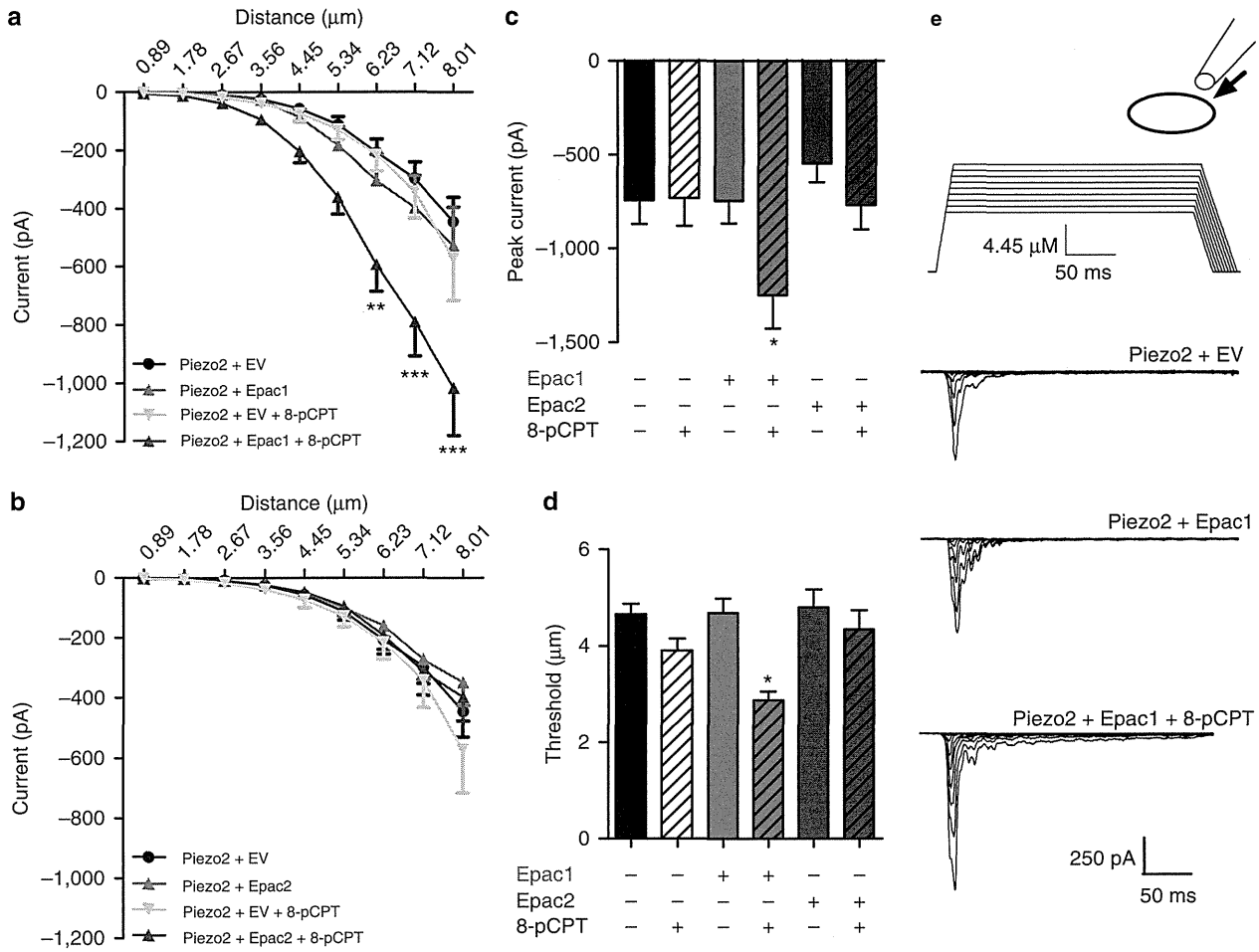

Figure 4 | Activation of Epac1 but not Epac2 sensitizes mechanically evoked Piezo2 currents. HEK293a cells were transfected with constructs encoding Piezo2+ empty pcDNA3 (EV, +8-pCPT, $n=21$; +vehicle, $n=38$), and (**a**) Piezo2+Epac1-YFP (+8-pCPT, $n=26$; +vehicle, $n=30$), or (**b**) Piezo2+Epac2-YFP (+8-pCPT, $n=17$, +vehicle, $n=23$). 8-pCPT (specific Epac activator) or vehicle was added and cells were voltage clamped at −70 mV in whole-cell configuration. (**a/b**) Mechanically evoked currents were elicited by increasing displacement of the cell membrane in ~0.9 μm increments. (**c**) Peak current elicited by the largest mechanical stimulus before whole-cell configuration was lost. (**d**) Threshold of activation was determined as the mechanical stimulus that elicited a current >20 pA. (**e**) Exemplar traces of currents in response to increasing membrane deformation of HEK293a cells expressing Piezo2+EV, Piezo2+Epac1 and Piezo2+Epac1+8-pCPT. All data are expressed as mean ± s.e.m. (**a–b**) Data were analysed using two-way analysis of variance followed by the Bonferroni *post hoc* test. $^*P<0.05$, $^{**}P<0.01$, $^{***}P<0.001$. In **c** and **d** '*' indicates significant difference compared with all other groups analysed by one-way analysis of variance followed by the Bonferroni *post hoc* test.

not change WDR neuron firing responses evoked by any mechanical stimuli (Fig. 6c).

The enhanced responses to mechanical stimuli could be mediated via changes in electrical excitability or at the level of mechanotransduction. Intraplantar 8-pCPT administration did not change WDR responses evoked by electrical activation of Aβ, Aδ or C fibres (Fig. 6d). Moreover, no changes in input, post-discharge or wind-up were observed (Fig. 6d). Both afferent electrical and central excitability are unaffected by 8-pCPT in line with our observation that 8-pCPT-induced allodynia is unaffected in mice deficient for DRG expression of voltage-gated sodium channels Nav1.7, Nav1.8 or Nav1.9 (Supplementary Fig. S4). Intraplantar injection of 6-Bnz-cAMP activates PKA and enhanced C-fibre-evoked WDR responses as well as input (a measure of afferent drive) but did not change electrically evoked Aβ- or Aδ-mediated WDR responses (Fig. 6e). Moreover post-discharge or wind-up were not changed by 6-Bnz-cAMP (Fig. 6e). Intraplantar vehicle injection did not induce any changes in electrically evoked WDR responses (Fig. 6f). These data indicate that 8-pCPT enhances responses to mechanical stimuli independent of changes in electrical excitability.

Epac1-mediated allodynia is Nav1.8+ nociceptor independent. Nav1.8+ sensory neurons comprise 85% of nociceptors and are essential for detecting noxious mechanical stimuli as well as for development of inflammatory hyperalgesia, but not neuropathic pain[24]. To test whether Nav1.8+ sensory neurons are required for 8-pCPT-induced mechanical allodynia, we used diphtheria toxin to kill these sensory neurons (*Nav1.8-DTA*[24]). As reported[24], baseline sensitivity to touch was similar in WT and Nav1.8-DTA mice (Fig. 7a). Importantly, the course of 8-pCPT-induced mechanical allodynia in mice in which Nav1.8 nociceptors were ablated was indistinguishable from control littermates (Fig. 7a). The absence of an effect of Nav1.8 nociceptor depletion on 8-pCPT-induced mechanical allodynia was independent of the dose of 8-pCPT; at any dose of 8-pCPT tested (12.5 pmol per paw–12.5 nmol per paw) mice showed no

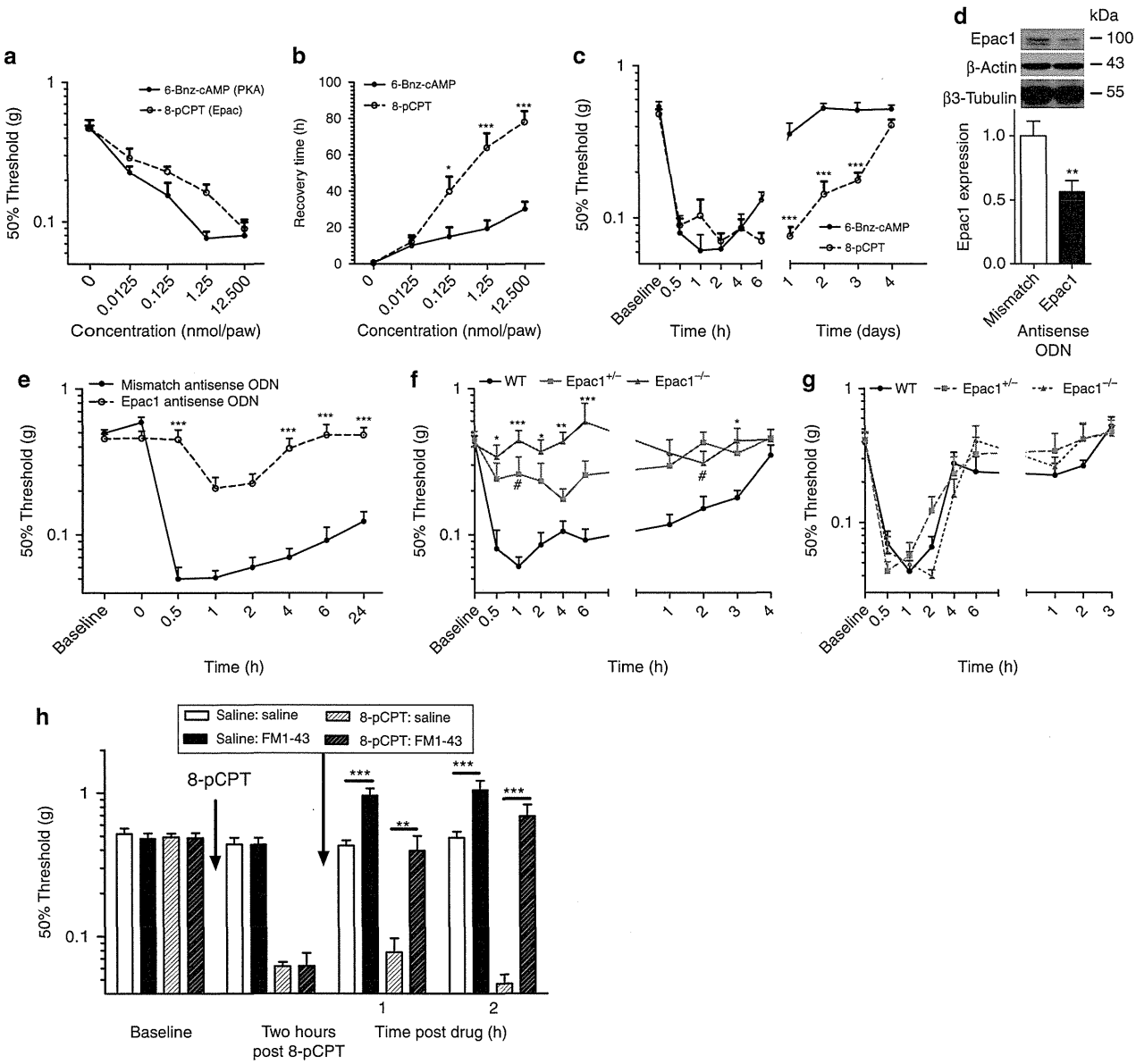

Figure 5 | The selective Epac activator 8-pCPT induces an Epac1-dependent long-lasting allodynia *in vivo*. Different doses of 8-pCPT (specific Epac activator; $n=4-8$) or 6-Bnz-cAMP (specific PKA activator; $n=4-8$) were injected intraplantarly and (**a**) 50% threshold to von Frey was determined 30 min after administration of drug. (**b**) Duration of 6-Bnz-cAMP or 8-pCPT-induced mechanical allodynia determined as the earliest time point in which 50% threshold is equal or higher than the average baseline 50% threshold ± 2x standard deviation ($n=4$–8). Time course of (**c**) mechanical hypersensitivity after intraplantar injection of 8-pCPT or 6-Bnz-cAMP (12.5 nmol per paw, $n=8$). (**d–e**) Epac1 antisense or mismatch antisense ODN were administered intrathecally once every two days for three times. (**d**) Two days after the last injection L2-L5 DRG Epac1 protein levels were determined by western Blot ($n=4$). (**e**) Time course of 8-pCPT-induced allodynia using von Frey in antisense ODN-treated animals ($n=8$). Repeated measures one-way analysis of variance: ODN treatment: $P<0.001$; time: $P<0.001$; interaction: $P<0.001$. (**f**) Time course of intraplantar 8-pCPT-induced allodynia (12.5 nmol per paw) in WT ($n=12$), *Epac1*+/− ($n=8$), and *Epac1*−/− ($n=8$) mice. Statistical analysis showed a genotype effect ($F(2, 25)=13,053$, $P<0.01$) and *post hoc* analysis shows that *Epac1*−/− ($P<0.001$) as well as *Epac1*+/− ($P<0.05$) significantly differed from WT mice. (**g**) Time course of intraplantar 6-Bnz-cAMP-induced mechanical allodynia (12.5 nmol per paw) in WT ($n=8$), *Epac1*+/− ($n=6$), *Epac1*−/− ($n=8$) mice. (**h**) Mice received intraplantar injection of 8-pCPT or vehicle and sensitivity of the mechanical stimulation was determined after 2 h. At this time point mice received an injection of FM1-43, or vehicle and threshold to mechanical stimulation was determined 1 and 2 h after injection. Data are expressed as mean ± s.e.m. Data were analysed using two-way analysis of variance followed by the Bonferroni *post hoc* test. (**d**) Data are analysed by *t*-test $^*P<0.05$, $^{**}P<0.01$, $^{***}P<0.001$. In f '#' indicates $P<0.05$ compared to WT mice.

notable difference in magnitude (Fig. 7b) or duration (Fig. 7c) of mechanical allodynia in *Nav1.8-DTA* mice compared with control littermates.

In contrast to nociceptor-independent mechanical allodynia induced by Epac activation, we found that PKA activation could sensitize mechanosensation through effects on Nav1.8+ nociceptors. Increasing doses of 6-Bnz-cAMP induced mechanical hypersensitivity that increased in magnitude and duration. The magnitude as well as the duration of 6-Bnz-cAMP-induced mechanical hypersensitivity was severely reduced in

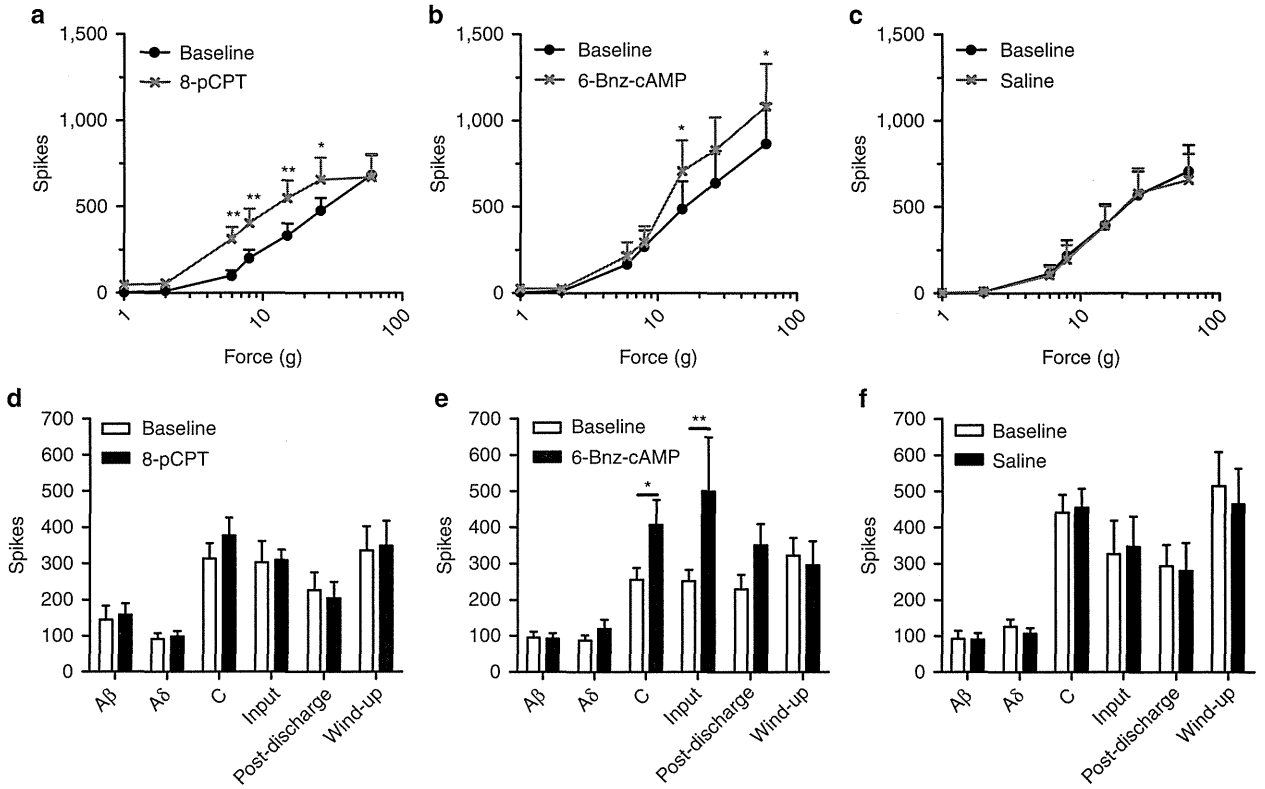

Figure 6 | *In vivo* electrophysiology of WDR neuron firing response after intraplantar 8-pCPT or 6-Bnz-cAMP. Evoked responses to von Frey filaments before and after administration of (**a**) 8-pCPT ($n=8$), (**b**) 6-Bnz-cAMP ($n=8$), or (**c**) saline ($n=7$). 8-pCPT shifted the stimulus-response curve to the left and enhanced responses to innocuous von Frey, while 6-Bnz-cAMP only enhanced response of von Frey >16 g. Responses to transcutaneous electrical stimulation of the receptive field before and after intraplantar injection of (**d**) 8-pCPT ($n=8$), (**e**) 6-Bnz-cAMP ($n=9$), or (**f**) saline ($n=7$). Data are expressed as mean ± s.e.m. (**a–c**) Data were analysed using two-way analysis of variance followed by the Bonferroni *post hoc* test. (**d–f**) Data are analysed by t-test $^{*}P<0.05$, $^{**}P<0.01$.

Nav1.8-DTA mice at all doses tested (12.5 pmol per paw–12.5 nmol per paw) (Fig. 7d,e). These data indicate that the PKA-dependent 6-Bnz-cAMP-induced mechanical hypersensitivity was almost completely absent in nociceptor-depleted mice. The highest dose (12.5 nmol per paw) used induced some mechanical hypersensitivity in nociceptor-depleted mice, but was significantly less intense and shorter than in control littermates (Fig. 7f).

Piezo2 is required for 8-pCPT-induced allodynia. We tested whether sensitization of Piezo2 contributes to 8-pCPT-induced allodynia. Intrathecal injection of antisense oligonucleotides (ODN) results in their concentration in DRG neurons, where RNA–DNA hybrids are degraded by RNase H; this approach to downregulating gene expression has been used in a variety of studies.[25] However, possible effects of antisense ODN in other cells within the spinal cord and DRG cannot be excluded. Intrathecal injection of a mixture of three different Piezo2 antisense ODN reduced Piezo2 mRNA expression in L2-L5 DRG by ~26%, 2 days after the last injection of antisense ODN (Fig. 7g). The reduction of DRG Piezo2 mRNA expression was associated with an increase in baseline thresholds to mechanical stimulation (Fig. 7h). 8-pCPT-induced mechanical allodynia was attenuated in Piezo2 antisense ODN-treated animals compared with mismatch ODN-treated mice (Fig. 7h). The partial reduction in Piezo2 mRNA is consistent with the behavioural effect of Piezo2 antisense treatment on 8-pCPT-induced allodynia.

Role of Piezo2 in touch sensation and allodynia. As Piezo2 antisense ODN treatment reduced Epac-mediated allodynia, we examined whether Piezo2 contributes to neuropathy induced allodynia and whether Piezo2 is involved in touch perception. Piezo2 antisense ODN mixture reduced Piezo2 mRNA expression in L2-L6 DRG by ~35% as measured 1 day after the last injection of Piezo2 antisense ODN, with no effect on Piezo1 levels (Fig. 7i). Piezo2 antisense ODN did not affect motor behaviour (Supplementary Fig. S5a). However, the reduction of Piezo2 mRNA expression was associated with an increase in 50% threshold to light mechanical stimulation to the hind paw (Fig. 7j). By contrast, responses to noxious mechanical stimulation or noxious heat were similar to mismatched control ODN-treated mice (Supplementary Fig. S5b,c).

To investigate the role of Piezo2 in neuropathy-induced allodynia, a unilateral L5 nerve transaction (L5 SNT) or a sciatic nerve ligation (chronic constriction injury (CCI)) was performed in mice to induce neuropathic pain. In both models mice developed mechanical allodynia in the ipsilateral paw, while mechanical thresholds to touch in the contralateral paw were unaffected (Fig. 8a–e). In the L5 SNT model, mice were treated intrathecally with Piezo2 antisense ODN starting at day 15. Piezo2 antisense treatment significantly attenuated L5 SNT-induced allodynia compared with mismatch-treated mice (Fig. 8a). Piezo2 antisense ODN treatment also increased thresholds to touch compared with mismatch antisense-treated mice at the unaffected contralateral paw (Fig. 8a). In the CCI model of neuropathic pain, multiple intrathecal Piezo2 antisense injections also significantly

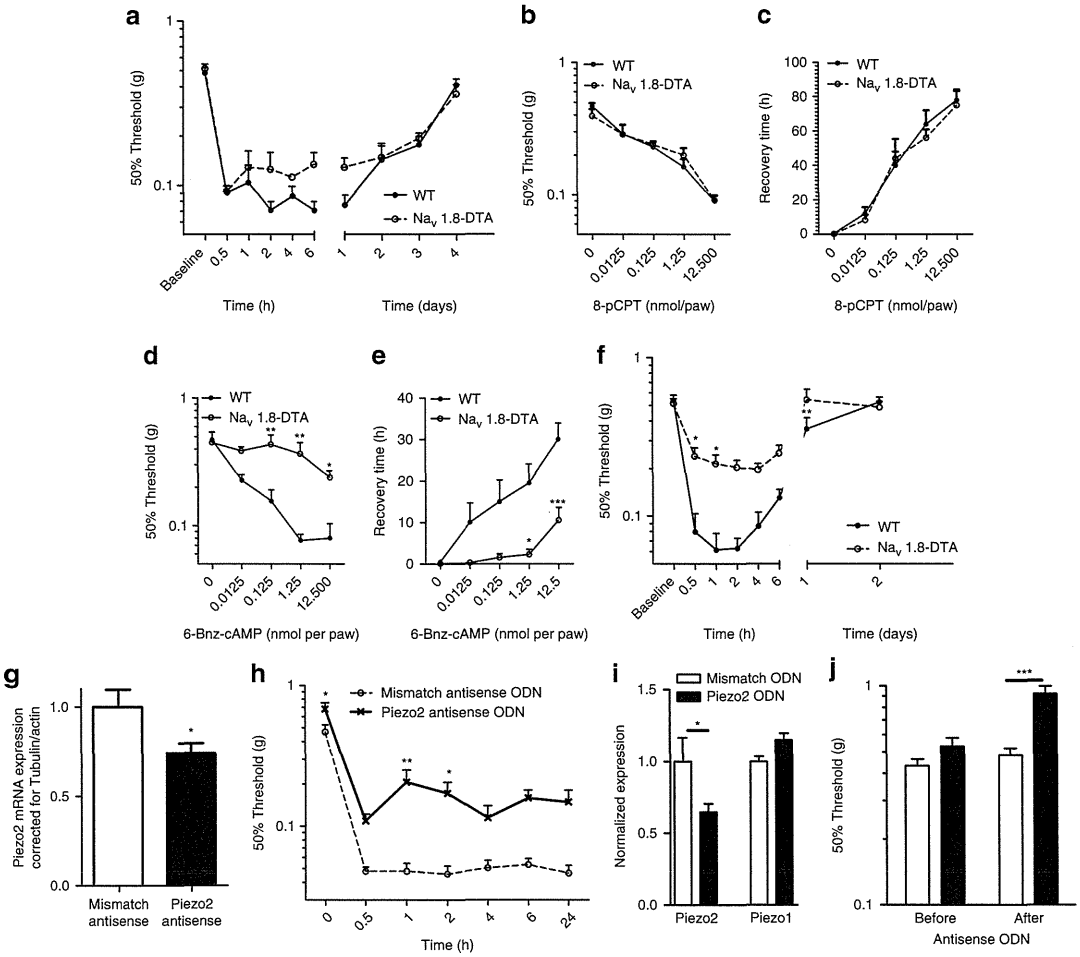

Figure 7 | Epac signalling-mediated allodynia is Piezo2 dependent and does not require Nav1.8 expressing nociceptors. WT and nociceptor-depleted mice *(Nav1.8-DTA)* received an intraplantar injection of 8-pCPT (12.5 nmol per paw) and time course of (**a**) allodynia ($n=8$) was determined. WT and *Nav1.8-DTA* mice received different doses of 8-pCPT (**b**, $n=4$-8) or 6-Bnz-cAMP (**d**, 6-Bnz-cAMP, $n=4$-8) and mechanical sensitivity was determined 5 h after intraplantar injection. Duration of 8-pCPT (**c**, $n=4$-8) or 6-Bnz-cAMP-induced (**e**, $n=4$-8) mechanical allodynia determined as the earliest time point in which the 50% threshold is equal or higher than the average baseline 50% threshold—2x standard deviation. (**f**) Time course of 6-Bnz-cAMP-induced (12.5 nmol per paw) allodynia ($n=8$). Repeated measures of allodynia: genotype: $P<0.001$, time: $P<0.001$, interaction: $P<0.05$. (**g**–**h**) Piezo2 or mismatch antisense ODNs were administered intrathecally 5, 3, 2, and 1 day before behavioural experiments. (**g**) Two days after the last injection L2-L5 DRG Piezo2 mRNA levels were determined by quantitative RT-PCR. (**h**) Time course of 8-pCPT-induced allodynia was determined using von Frey. (**i**) To verify role of Piezo2 in touch perception, one day after the last antisense ODN injection L2-L6 DRG Piezo1/2 mRNA expression levels were determined by quantitative RT-PCR. (**j**) Sensitivity to touch was determined using Von Frey filaments. Data are expressed as mean ± s.e.m. (**a**–**f**, **h**)Data were analysed using two-way analysis of variance followed by the Bonferroni *post hoc* test. (**g**,**i**) Data are analysed by *t*-test. (**j**) Data were analysed using one-way analysis of variance followed by the Bonferroni *post hoc* test. $^*P<0.05$, $^{**}P<0.01$, $^{***}P<0.001$.

attenuated CCI-induced mechanical allodynia (Fig. 8b). At the unaffected contralateral paw, Piezo2 antisense ODN treatment also increased thresholds to touch (Fig. 8b). Although Piezo2 antisense ODN increased mechanical thresholds both at the ipsi- and contralateral paw in both models of neuropathic pain, Piezo2 antisense ODN reduced the neuropathic pain-induced difference in mechanosensitivity between the contra and ipsilateral paw (Fig. 8c).

Twenty-four hours after the last Piezo2 antisense ODN injection, Piezo2 mRNA was reduced by more than 50% in both the ipsilateral and contralateral DRGs in both models of neuropathic pain (Fig. 8d,e). Piezo1 DRG mRNA expression levels were unaffected after Piezo2 antisense ODN treatment (Supplementary Fig. 6). These data show that transcription of Piezo1 and Piezo2 are unaffected by nerve damage as no difference between the ipsi and contralateral paw was observed.

Discussion

The molecular basis of touch and mechanical allodynia is poorly understood. Here, we show that activation of Epac1 contributes to the development of allodynia associated with neuropathic pain. Epac1 signalling produces allodynia involving Piezo2-mediated mechanotransduction in low threshold mechanosensitive sensory neurons independently of Nav1.8 + nociceptors. Epac1 signalling enhances mechanically evoked Piezo2-mediated currents in a heterologous expression system, as well as endogenous rapidly adapting mechanically gated currents in sensory neurons. We also

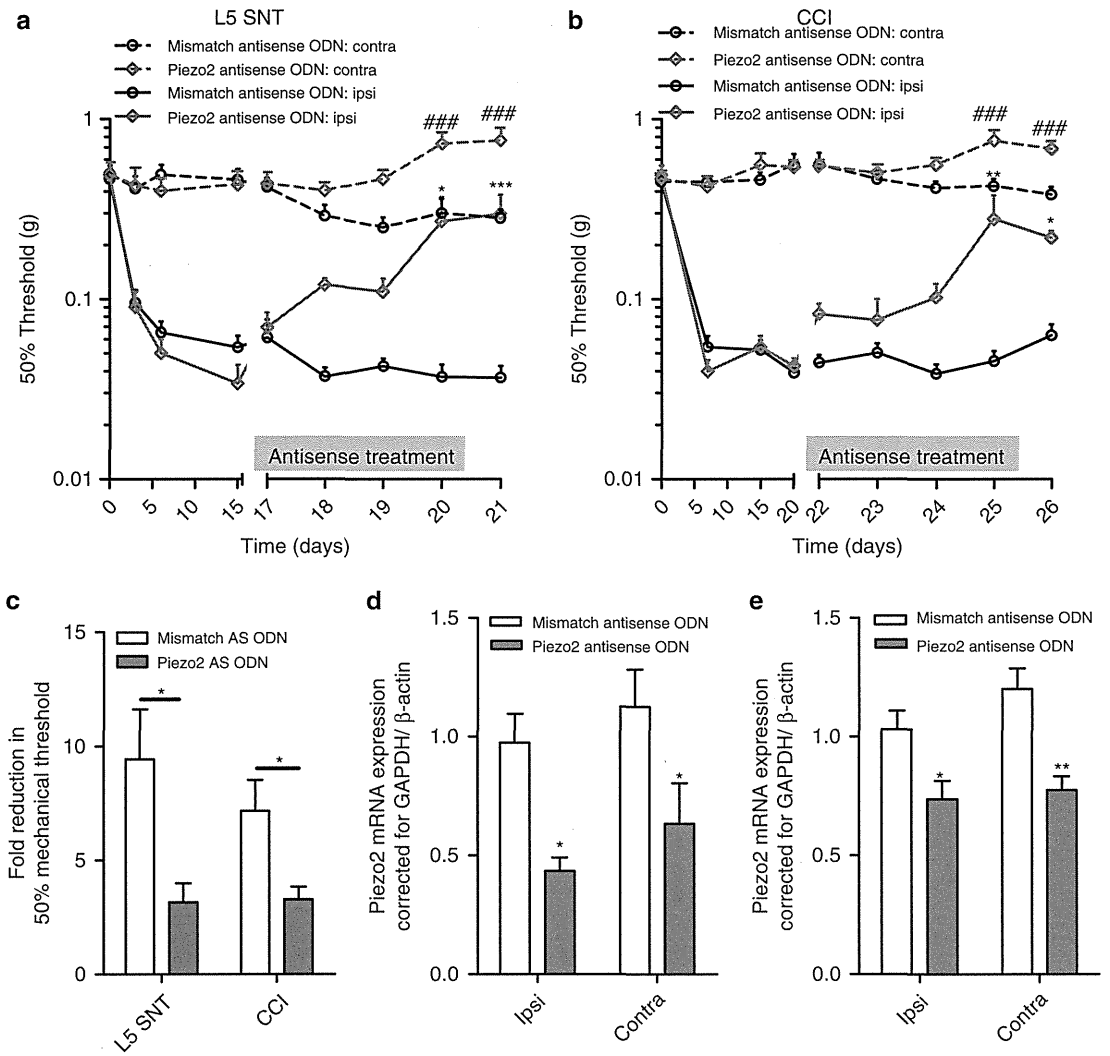

Figure 8 | Piezo2 is required for allodynia in two models of chronic neuropathic pain. Mice were subjected to a unilateral L5 spinal nerve transaction (L5 SNT; **a**) or to a unilateral chronic constriction injury of the sciatic nerve (CCI; **b**). The 50% threshold to von Frey was measured at the ipsilateral and contralateral paw. Piezo2 (L5 SNT, $n=5$; CCI, $n=6$) or mismatch antisense (L5 SNT, $n=9$; CCI, $n=10$) was administered after full development of allodynia (2-3 weeks after operation) as indicated by the grey bars. (**c**) Fold reduction of 50% threshold to von Frey of the ipsilateral paw compared the contralateral paw in both models of neuropathic pain at day 21 (L5 SNT; $n=5$-9) or 26 (CCI; $n=6$-10). Piezo2 mRNA expression in the ipsi- and contralateral DRG expression was measured 1 day after the last antisense ODN administration(**d**, L 5 SNT, $n=5$-9; **e**, CCI, $n=6$-10). Two-way one-way analysis of variance showed a significant overall reduction in Piezo2 mRNA $P<0.01$. Data are expressed as mean ± s.e.m. Data were analysed using two-way analysis of variance followed by the Bonferroni *post hoc* test. $^{*}P<0.05$, $^{**}P<0.001$, $^{***}P<0.001$. In **a** and **b** '###'indicate $P<0.001$ compared to the contralateral paw of mismatch antisense ODN treated mice.

show that Piezo2 is likely to have a role in the detection of light touch and the development of allodynia.

We found that Epac1 activation enhances mechanically evoked currents in low threshold mechanosensitive sensory neurons, many of which are associated with touch. Interestingly, this subset of sensory neurons lose their mechanically evoked currents after treatment with Piezo2 siRNA[4]. Mechanically evoked Piezo2 currents are enhanced upon Epac1 activation and *in vivo* activation of Epac1 produces a Piezo2-dependent allodynia that can be blocked by the permeant mechanosensory channel blocker FM1-43. PKA-mediated effects on mechanosensation do not involve mechanotransduction but act through sensitization of nociceptor electrical excitability[1], and activation of PKA does not enhance Piezo2 currents in HEK293 cells. Overall, Epac1 signalling appears to selectively enhance Piezo2-mediated mechanotransduction contributing to allodynia.

The contribution of cAMP signalling to sensitization of sensory neurons is well described. However, the role of the cAMP-sensor protein Epac1 in peripheral pain pathways is relatively unexplored. Intraplantar injection of the Epac agonist 8-pCPT has been shown to lead to a decrease in mechanical nociceptive thresholds in rats via a PKCε-dependent pathway[23]. We have found that activation of Epac1 leads to long-lasting allodynia, while activation of PKA induces a transient mechanical hypersensitivity linked to enhanced electrical excitability. The Epac1-mediated development of allodynia required a different subset of sensory neurons compared with those activated by PKA. PKA-mediated mechanical hyperalgesia requires

Nav1.8+ nociceptors, while Epac-mediated allodynia was independent of these sensory neurons. Earlier findings showed that 8-pCPT enhanced noxious mechanosensation in IB4+ sensory neurons,[23] that can be either Nav1.8+ or Nav1.8−. Interestingly, 8-pCPT-induced thermal hyperalgesia is almost completely absent in Nav1.8 nociceptor-depleted mice (Supplementary Fig. S7). Thus, these data indicate that Epac activation in non Nav1.8 expressing cells selectively leads to mechanical allodynia, while Epac activation in Nav1.8+ neurons causes thermal hyperalgesia or mechanical hyperalgesia in IB4+ neurons. Consistent with these observations, Nav1.8+ nociceptors are not required for the development of allodynia in a neuropathic pain model[24], and the development of allodynia is also attenuated in *Epac1*+/− and *Epac1*−/− mice in a neuropathic pain model. The sensory neuron subset-specific role of Epac1 signalling is also highlighted by the fact that reduction of an endogenous inhibitor of Epac1, G protein-coupled receptor kinase 2 in Nav1.8 expressing neurons, enhanced 8-pCPT-induced thermal hyperalgesia.[26] Finally, we have found that downstream signalling cascades activated by inflammatory mediators and linked to mechanical hyperalgesia rather than allodynia, such as PKC and PKA, do not alter Piezo2 currents. In contrast, increased intracellular calcium concentrations strongly potentiated hPiezo currents.

Although Aβ fibre-associated pain is little studied, Aβ nociceptors exist[27], and allodynia has been linked with Aβ sensory neuron activation[28]. It is also possible that besides the role of Epac1–Piezo2 in peripheral sensitization, other (spinal) processes induced by nerve damage link Aβ fibres to pain pathways.

The question arises whether Epac1 activation acts directly or indirectly on Piezo2. Epac signalling,has been shown to cause PKCε translocation to the cell membrane, and PLCε activation that could potentiate Piezo2-mediated currents through elevated intracellular calcium[29]. Further research to elucidate the mechanisms underlying Epac1-mediated Piezo sensitization and allodynia is required.

Characterization of human Piezo2 showed that this channel has similar properties to mouse Piezo2, already linked to rapidly adapting mechanically gated currents in DRG neurons. Consistent with this, antisense-mediated Piezo2 knockdown decreases mRNA expression and sensitivity to touch. This contrasts with the role of Piezo in *Drosophila*, which has no role in touch[30]. Intrathecal Piezo2 antisense ODN treatment attenuates mechanical allodynia induced by Epac1 activation or neuropathy.

In conclusion, these findings are the first to demonstrate a role for the cAMP-sensor Epac1 in mechanical allodynia in neuropathic pain and highlight Epac1 as a modulator of Piezo2, a mechanotransducer that we show here to be linked to mechanical allodynia and touch. These data suggest that the Epac1–Piezo2 axis is an important regulator of allodynia and is a potential therapeutic target for the treatment of neuropathic pain.

Methods

Animals. All behavioural tests were approved by the United Kingdom Home Office Animals (Scientific Procedures) Act 1986. *Epac1*+/−, *Epac1*−/− and their WT control littermates were from a C57BL/6 and CBA mixed background[31]. *Nav1.8*−/−, *Nav1.9*−/− C57Bl/6 and WT control littermates were used[32,33]. Nav1.7 deletion in all sensory neurons was accomplished by using heterozygous advillin-Cre/homozygous floxed Nav1.7 mice[34]. Ablation of Nav1.8 neurons was achieved by crossing heterozygous Nav1.8-Cre mice with homozygous eGFP-diphtheria toxin (DTA) mice[24]. For behavioural testing, mice aged 8–12 weeks were used. *In vivo* spinal cord electrophysiology was performed on Sprague-Dawley rats.

Measurement of mechanical allodynia and thermal hyperalgesia. The development of thermal hyperalgesia was measured with the Hargreave's apparatus[35]. Mechanical hyperalgesia was measured using von Frey hairs (Stoelting, Wood Dale, USA), and the 50% paw withdrawal threshold was calculated using the up-and-down method[36]. Noxious mechanical sensitivity was assessed using Randall Selitto apparatus[37]. Baseline withdrawal latencies or mechanical thresholds were averaged over at least three measurements before intraplantar injection of compounds or surgery. All experiments were performed in a blinded manner.

Drugs and preparation. Mice received an intraplantar injection of 2.5 µl of the Epac activator 8-(4-Chlorophenylthio)-2′-methyl-cAMP (8-pCPT; Biolog Life Science Institute, Bremen, Germany), or N6-Benzoyl-cAMP salt (6-Bnz-cAMP, Biolog Life Science Institute)[26]. As a control, a similar amount of vehicle was injected. FM1-43 (2 nmol µl^{-1}) was dissolved in saline and injected intraplantarly (2.5 µl) 2 h after 8-pCPT injection[20].

***In vivo* antisense ODN treatment.** Antisense ODNs[38] dissolved in saline (Epac1: 10 µg per 5 µl; Piezo2 mixture: 15 µg per 5 µl) were injected intrathecally[39]. Epac1 antisense ODN: mice were injected with Epac1 antisense ODN at 5, 3 and 1 days before injection of 8-pCPT. Piezo2 antisense ODN: mice were injected with Piezo2 antisense ODN at day 5, 3, 2 and 1 days before injection of 8-pCPT. During chronic neuropathic pain, Piezo2 antisense ODN were intrathecally injected daily. 24–48 h after the last injection DRGs were isolated. All antisense ODN had a phosphorothioate backbone.
The following ODN were used:
Epac1: 5′-AACTCTCCACCCTCTCCCA-3′; mismatch: 5′-ACATTCCACCCTC CTCCAC-3′
Piezo2: 5′-GTCCTTCCAGCCACATCTTCT-3′ + 5′-CCTTCTACCACCTCCT CCTC-3′ + 5′-ACCACCCGACCTCACAAGCA-3′; mismatch: 5′-TCCGTCTCG CACAACTCTCTT-3′ + 5′-CTTCTACCACTCCTCCCTCC-3′ + 5′-ACACCAC CCTCGCCAACGAA-3′.

Neuropathic pain models. A unilateral L5 nerve transaction (L5 SNT) was introduced in anaesthetized mice[40]. The L5 transverse process was removed using a blunt fine forceps and the left L5 spinal nerve was cut.
CCI was introduced to mice according to a modified protocol used for rats[41]. In anaesthetized mice, the left sciatic nerve was exposed at mid-thigh level and three loose ligatures were made around the nerve.

***In vivo* rat spinal cord electrophysiology.** Experiments were performed on anaesthetized male Sprague-Dawley rats (Central Biological Services, UCL), as previously described[42]. Saline, 8-pCPT or 6-Bnz-cAMP was administered into the receptive field of the cell (hind paw). The results were calculated as maximum change from the pre-drug control values for each response per neuron. See for full details Supplementary Methods.

Expression plasmids. The full-length hPiezo2 open reading frame was cloned into pcDNA3 (Invitrogen) in two sections to give the construct 'PIEZO2 in pcDNA3'. The 2,752 amino-acid PIEZO2 protein encoded by the construct is identical to NP_071351, except for containing SNPs rs7234309 (I) and rs3748428 (I). Finally, a polio IRES-eGFP fragment was PCR amplified from clone JC5 (ref. 45) and ligated into 'PIEZO2 in pcDNA3' to give the final construct 'PIEZO2-IRES-eGFP'. The coding sequence of the PIEZO2 construct has been sequenced entirely and has been submitted to GenBank under accession number JN790819. For Epac1/2 overexpression studies YFP-Epac1 and YFP-Epac2 were used[44].

Culture of DRG neurons. Adult mice DRG neurons were dissected out and subsequently digested in an enzyme mixture containing Ca^{2+}- and Mg^{2+}-free HBSS, 5 mM HEPES, 10 mM glucose, collagenase type XI (5 mg ml^{-1}) and dispase (10 mg ml^{-1}) for 1 h before mechanical trituration in DMEM + 10% heat-inactivated fetal bovine serum. Cells were centrifuged for 5 min at 800 r.p.m., resuspended in DMEM containing 4.5 g l^{-1} glucose, 4 mM L-glutamine, 110 mg l^{-1} sodium pyruvate, 10% fetal bovine serum, 1% penicillin–streptomycin (10,000 i.u. ml^{-1}), 1% glutamax, 125 ng ml^{-1} nerve growth factor, and plated on poly-L-lysine- (0.01 mg ml^{-1}) and laminin- (0.02 mg ml^{-1}) coated 35-mm dishes. Neurons were used 24 h after plating.

Cell culture. HEK293a cells were cultured in DMEM supplemented with 10% fetal calf serum (FCS). Plasmid DNA was transiently transfected into the cells using Lipofectamine 2000 (Invitrogen) in a ratio of 1 µg DNA:2.5 µl Lipofectamine 2000 according to the manufacturer's instructions. Electrophysiology recordings were made 48 h post transfection.

Electrophysiology. Neurons whose cell bodies were not in contact with those of other neurons and transfected HEK293a cells tagged with fluorescent proteins were selected for recording. Currents were recorded using Axopatch 200B and Multiclamp 700 amplifiers (Axon Instruments, Molecular Devices Inc.). Pipettes were pulled from borosilicate glass capillaries with a P-97 puller (Sutter Instrument Co.)

with resistances of 2–4 MΩ. Currents were digitized with the Digidata 1322A and 1440A data acquisition systems (Axon Instruments, Molecular Devices Inc.). Data were captured using PClamp 8.1 & 10 software and analysed using ClampFit 10.2 (Axon Instruments). Currents were low-pass filtered at 5 kHz and sampled at 10 kHz. Capacity transients were cancelled, however, series resistance were not compensated. Voltages were not corrected for liquid junction potentials. Recordings were performed at room temperature. Recordings were carried out in the perforated patch configuration. The pipette solution contained (in mM) 110 CH_3COOK, 30 KCl, 5 NaCl, 1 $MgCl_2$ and 10 HEPES (pH corrected to 7.35 using KOH, osmolarity: ~310 mOsm with sucrose). 205 Mg per mililitre of fresh amphotericin B was added to this solution before recording. The bath solution contained (in mM): 140 NaCl, 4 KCl, 2 $CaCl_2$, 1 $MgCl_2$, 5 glucose and 10 HEPES (pH 7.4 adjusted using NaOH, osmolarity: ~320 mOsm with sucrose). 8-pCPT was added to the bath solution after establishment of a stable response to a 0.008 Hz mechanical stimulus. In HEK293 cells expressing Piezo1/2 either bath solution or 8-pCPT was added to the bath solution. Recordings were made 20–50 min after the addition of 8-pCPT at room temperature. For experiments in which cytosolic Ca^{2+} concentration was fixed, the conventional whole-cell configuration was used. Whole-cell patch clamp solution contained (in mM) KCl (130), $MgCl_2$ (2.5), $CaCl_2$ (1.94 or 4.63 to give 50 nM or 1 μM free Ca^{2+}), EGTA (5) K-ATP (3) HEPES (5) and pH 7.4 KOH (osmolarity was set to 310 mOsm with sucrose).

Mechanical stimulation. Mechanical stimulation of cell bodies was achieved using a heat-polished glass pipette (tip diameter ~2 μm), controlled by a piezo-electric crystal drive (Siskiyou MXPZT-300 series or Burleigh LSS-3000 series), positioned at an angle of about 70° to the surface of the dish. The probe was positioned so that a ~x μm (x = 10–14 μm) movement did not visibly contact the cell but that a x + 1 μm stimulus produced an observable membrane deflection. The probe was moved at a speed of 1 μm ms^{-1} and the stimulus was applied for 250 ms. A series of mechanical steps in ~1 (HEK cells) or ~2 μm (DRG neurons) increments were applied. Criteria for classifying adaptation kinetics of rapidly adapting mechanosensitive currents (RA) in DRG neurons had a decay kinetic that was best described by a bi-exponential fit[5]. Kinetics of adaptation to the mechanical stimuli were fitted with a standard mono exponential decay with the equation below using PClamp 10.2.

$$f(t) = \sum_{i=1}^{n} A_i e^{-t/\tau_i} + C$$

The fit solves for the amplitude A, the time constant τ, and the constant y-offset C for each component i.

Western blot analysis. DRG cultures were homogenized in ice-cold RAL lysis buffer (200 mM NaCl, 50 mM Tris–HCl (pH 7.5), 10% glycerol, 1% NP-40, 2 mM sodium orthovanadate, 2 mM phenylmethylsulfonyl fluoride and protease inhibitor mix (Sigma-Aldrich, p3840, 1:100)). Proteins were separated by SDS–polyacrylamide gel electrophoresis and transferred to PVDF membranes (Millipore, Bedford, MA, USA). Blots were stained with mouse-anti-Epac1 and as loading control rabbit-anti-β-actin or the neuron-specific mouse-anti-β3-tubulin (all cell signalling). Subsequently, blots were incubated with goat anti-mouse-peroxidase or donkey-anti-rabbit IgG + IgM (H + L) (GE Healthcare) and developed by enhanced chemiluminescence plus (Amersham Int.).

mRNA isolation and real-time PCR. Lumbar DRGs (L2-L5) were isolated and total RNA was isolated with RNeasy Mini Kit (Qiagen) in accordance with the manufacturer's instructions. Reverse transcription was performed with 1 μg of RNA by using iScript Select cDNA Synthesis Kit (Invitrogen). Real-time quantitative PCR was then performed with iQ SYBR Green Supermix (Invitrogen). The following primer pairs were used:

Epac1: 5′-gTgTTggTgAAggTCAATTCTg-3′ (forward), 5′-CCACACCACgggCATC-3′ (reverse)

Epac2: 5′-TgTTAAAgTgTCTgAgACCAgCA-3′ (forward), 5′-AAAggCTgTCCCAATTCCCAg-3′ (reverse)

Piezo1: 5′-CTACAAATTCgggCTggAg-3′ (forward), 5′-TCCAgCgCCATggATAgT-3′ (reverse)

Piezo2: 5′-CCAAgTAgCCCATgCAAAAT-3′ (forward), 5′-gCATAACCCTgTgCCAgATT-3′ (reverse)

β-Actin: 5′-AgAgggAAATCgTgCgTgAC-3′ (forward), 5′-CAATAgTgATgACCTggCCgT-3′ (reverse)

GAPDH: 5′-TgAAgCAggCATCTgAgg-3′ (forward), 5′-CgAAggTggAAgAgTgggAg-3′ (reverse)

Data analysis. Data are expressed as mean ± s.e.m. Measurements were compared using Student's t-test, one-way one-way analysis of variance (ANOVA), repeated measures, or two-way ANOVA followed by Bonferroni's analysis. A P-value of <0.05 was considered to be statistically significant.

References

1. Di Castro, A., Drew, L. J., Wood, J. N. & Cesare, P. Modulation of sensory neuron mechanotransduction by PKC- and nerve growth factor-dependent pathways. *Proc. Natl Acad. Sci. USA* **103,** 4699–4704 (2006).
2. Wood, J. N. & Eijkelkamp, N. Noxious mechanosensation-molecules and circuits. *Curr. Opin. Pharmacol.* **12,** 4–8 (2012).
3. Costigan, M., Scholz, J. & Woolf, C. J. Neuropathic pain: a maladaptive response of the nervous system to damage. *Annu. Rev Neurosci.* **32,** 1–32 (2009).
4. Coste, B. *et al.* Piezo1 and Piezo2 are essential components of distinct mechanically activated cation channels. *Science* **330,** 55–60 (2010).
5. Quick, K. *et al.* TRPC3 and TRPC6 are essential for normal mechanotransduction in subsets of sensory neurons and cochlear hair cells. *Open. Biol.* **2,** 120068 (2012).
6. Hucho, T. & Levine, J. D. Signaling pathways in sensitization: toward a nociceptor cell biology. *Neuron* **55,** 365–376 (2007).
7. Bos, J. L. Epac proteins: multi-purpose cAMP targets. *Trends Biochem. Sci.* **31,** 680–686 (2006).
8. Wei, F. *et al.* Genetic elimination of behavioral sensitization in mice lacking calmodulin-stimulated adenylyl cyclases. *Neuron* **36,** 713–726 (2002).
9. Pierre, S., Eschenhagen, T., Geisslinger, G. & Scholich, K. Capturing adenylyl cyclases as potential drug targets. *Nat. Rev. Drug Discov.* **8,** 321–335 (2009).
10. Yajima, Y. *et al.* Differential involvement of spinal protein kinase C and protein kinase A in neuropathic and inflammatory pain in mice. *Brain Res.* **992,** 288–293 (2003).
11. Malmberg, A. B. *et al.* Diminished inflammation and nociceptive pain with preservation of neuropathic pain in mice with a targeted mutation of the type I regulatory subunit of cAMP-dependent protein kinase. *J. Neurosci.* **17,** 7462–7470 (1997).
12. Grandoch, M., Roscioni, S. S. & Schmidt, M. The role of Epac proteins, novel cAMP mediators, in the regulation of immune, lung and neuronal function. *Br. J. Pharmacol.* **159,** 265–284 (2010).
13. Gloerich, M. & Bos, J. L. Epac: defining a new mechanism for cAMP action. *Annu. Rev. Pharmacol. Toxicol.* **50,** 355–375 (2010).
14. Holz, G. G., Kang, G., Harbeck, M., Roe, M. W. & Chepurny, O. G. Cell physiology of cAMP sensor Epac. *J. Physiol.* **577,** 5–15 (2006).
15. McCarter, G. C., Reichling, D. B. & Levine, J. D. Mechanical transduction by rat dorsal root ganglion neurons *in vitro*. *Neurosci. Lett.* **273,** 179–182 (1999).
16. Drew, L. J., Wood, J. N. & Cesare, P. Distinct mechanosensitive properties of capsaicin-sensitive and -insensitive sensory neurons. *J. Neurosci.* **22,** RC228 (2002).
17. Drew, L. J. *et al.* Acid-sensing ion channels ASIC2 and ASIC3 do not contribute to mechanically activated currents in mammalian sensory neurones. *J. Physiol.* **556,** 691–710 (2004).
18. Hu, J. & Lewin, G. R. Mechanosensitive currents in the neurites of cultured mouse sensory neurones. *J. Physiol.* **577,** 815–828 (2006).
19. Hao, J. & Delmas, P. Multiple desensitization mechanisms of mechanotransducer channels shape firing of mechanosensory neurons. *J. Neurosci.* **30,** 13384–13395 (2010).
20. Drew, L. J. & Wood, J. N. FM1-43 is a permeant blocker of mechanosensitive ion channels in sensory neurons and inhibits behavioural responses to mechanical stimuli. *Mol. Pain* **3,** 1 (2007).
21. Kimitsuki, T. & Ohmori, H. Dihydrostreptomycin modifies adaptation and blocks the mechano-electric transducer in chick cochlear hair cells. *Brain Res.* **624,** 143–150 (1993).
22. Cho, H., Shin, J., Shin, C. Y., Lee, S. Y. & Oh, U. Mechanosensitive ion channels in cultured sensory neurons of neonatal rats. *J. Neurosci.* **22,** 1238–1247 (2002).
23. Hucho, T. B., Dina, O. A. & Levine, J. D. Epac mediates a cAMP-to-PKC signaling in inflammatory pain: an isolectin B4(+) neuron-specific mechanism. *J. Neurosci.* **25,** 6119–6126 (2005).
24. Abrahamsen, B. *et al.* The cell and molecular basis of mechanical, cold, and inflammatory pain. *Science* **321,** 702–705 (2008).
25. Ferrari, L. F., Chum, A., Bogen, O., Reichling, D. B. & Levine, J. D. Role of Drp1, a key mitochondrial fission protein, in neuropathic pain. *J. Neurosci.* **31,** 11404–11410 (2011).
26. Eijkelkamp, N. *et al.* Low nociceptor GRK2 prolongs prostaglandin E2 hyperalgesia via biased cAMP signaling to Epac/Rap1, protein kinase C{varepsilon}, and MEK/ERK. *J. Neurosci.* **30,** 12806–12815 (2010).
27. Djouhri, L. & Lawson, S. N. Abeta-fiber nociceptive primary afferent neurons: a review of incidence and properties in relation to other afferent A-fiber neurons in mammals. *Brain Res. Brain Res. Rev.* **46,** 131–145 (2004).
28. Zhu, Y. F. & Henry, J. L. Excitability of abeta sensory neurons is altered in an animal model of peripheral neuropathy. *BMC Neurosci.* **13,** 15 (2012).
29. Oestreich, E. A. *et al.* Epac and phospholipase cepsilon regulate Ca2+ release in the heart by activation of protein kinase cepsilon and calcium-calmodulin kinase II. *J. Biol. Chem.* **284,** 1514–1522 (2009).

30. Kim, S. E., Coste, B., Chadha, A., Cook, B. & Patapoutian, A. The role of *Drosophila* piezo in mechanical nociception. *Nature* **19,** 209–212 (2012).
31. Suzuki, S. *et al.* Differential roles of Epac in regulating cell death in neuronal and myocardial cells. *J. Biol. Chem.* **285,** 24248–24259 (2010).
32. Akopian, A. N. *et al.* The tetrodotoxin-resistant sodium channel SNS has a specialized function in pain pathways. *Nat. Neurosci.* **2,** 541–548 (1999).
33. Ostman, J. A., Nassar, M. A., Wood, J. N. & Baker, M. D. GTP up-regulated persistent Na+ current and enhanced nociceptor excitability require NaV1.9. *J. Physiol.* **586,** 1077–1087 (2008).
34. Minett, M. S. *et al.* Distinct Nav1.7-dependent pain sensations require different sets of sensory and sympathetic neurons. *Nat. Commun* **24,** 791 (2012).
35. Hargreaves, K., Dubner, R., Brown, F., Flores, C. & Joris, J. A new and sensitive method for measuring thermal nociception in cutaneous hyperalgesia. *Pain* **32,** 77–88 (1988).
36. Chaplan, S. R., Bach, F. W., Pogrel, J. W., Chung, J. M. & Yaksh, T. L. Quantitative assessment of tactile allodynia in the rat paw. *J. Neurosci. Methods* **53,** 55–63 (1994).
37. Minett, M. S. *et al.* Distinct Nav1.7-dependent pain sensations require different sets of sensory and sympathetic neurons. *Nat. Commun.* **3,** 791 (2012).
38. Lai, J. *et al.* Immunofluorescence analysis of antisense oligodeoxynucleotide-mediated 'knock-down' of the mouse delta opioid receptor *in vitro* and *in vivo*. *Neurosci. Lett.* **213,** 205–208 (1996).
39. Hylden, J. L. & Wilcox, G. L. Intrathecal morphine in mice: a new technique. *Eur. J. Pharmacol.* **67,** 313–316 (1980).
40. Mabuchi, T. *et al.* Pituitary adenylate cyclase-activating polypeptide is required for the development of spinal sensitization and induction of neuropathic pain. *J. Neurosci.* **24,** 7283–7291 (2004).
41. Bennett, G. J. & Xie, Y. K. A peripheral mononeuropathy in rat that produces disorders of pain sensation like those seen in man. *Pain* **33,** 87–107 (1988).
42. Dickenson, A. H. & Sullivan, A. F. Electrophysiological studies on the effects of intrathecal morphine on nociceptive neurones in the rat dorsal horn. *Pain* **24,** 211–222 (1986).
43. Shpacovitch, V. M. *et al.* Agonists of proteinase-activated receptor-2 modulate human neutrophil cytokine secretion, expression of cell adhesion molecules, and migration within 3-D collagen lattices. *J. Leukoc. Biol.* **76,** 388–398 (2004).
44. Gloerich, M. *et al.* Spatial regulation of cyclic AMP-Epac1 signaling in cell adhesion by ERM proteins. *Mol. Cell Biol.* **30,** 5421–5431 (2010).
45. Cox, JJ. *et al.* An SCN9A channelopathy causes congenital inability to experience pain. *Nature* **444,** 894–898.

Acknowledgements

N.E. was supported by a Rubicon fellowship of the Netherlands Organisation for Scientific Research. J.M.T. was supported by José Castillejo fellowship JC2010-0196 granted by the Spanish Ministry of Science and Innovation. J.J.C. is supported by an MRC Research Career Development Fellowship. J.N.W. GL U.O. and G.S.H. were supported by WCU grant R31-2008-000-10103-0 at SNU. This work was also supported by an EU IMI Europain grant and BBSRC LOLA grant (J.N.W., J.E.L.) and the Wellcome Trust (J.N.W., M.S.M.). We are greatly indebted to Sam Gossage for excellent technical assistance.

Author contributions

N.E. and J.W. designed and supervised experiments. N.E. performed most of the *in vivo* and *in vitro* experiments. J.L. performed experiments to characterize hPiezo2. G.H and G.L. supervised by U.O., and J.T. and J.C. cloned hPiezo. L.B. performed the *in vivo* electrophysiology under the supervision of A.D. M.G. helped with the overexpression studies. M.M. performed surgery. Y.I. provided the Epac1 −/− mice. F.Z. provided the Epac constructs. N.E. and J.W. wrote manuscript with contributions of all authors. N.E., J.L. and L.B. contributed to data analysis and all authors contributed to the discussions.

Additional information

Supplementary Information accompanies this paper at http://www.nature.com/naturecommunications

Competing financial interests: The authors declare no competing financial interests.

Reprints and permission information is available online at http://npg.nature.com/reprintsandpermissions/

How to cite this article: Eijkelkamp N. *et al.* A role for Piezo2 in EPAC1-dependent mechanical allodynia. *Nat. Commun.* 4:1682 doi: 10.1038/ncomms2673 (2013).

Balancing GRK2 and EPAC1 levels prevents and relieves chronic pain

Huijing Wang,[1,2] Cobi J. Heijnen,[3] Cindy T.J. van Velthoven,[1] Hanneke L.D.M. Willemen,[1] Yoshihiro Ishikawa,[4] Xinna Zhang,[5] Anil K. Sood,[5] Anne Vroon,[1] Niels Eijkelkamp,[1] and Annemieke Kavelaars[3]

[1]Laboratory of Neuroimmunology and Developmental Origins of Disease, University Medical Center Utrecht, Utrecht, The Netherlands. [2]Department of Pharmacology, Shanghai Medical College, Fudan University, Shanghai, People's Republic of China. [3]Neuroimmunology of Cancer Related Symptoms (NICRS) Laboratory, Department of Symptom Research, University of Texas M.D. Anderson Cancer Center, Houston, Texas, USA. [4]Cardiovascular Research Institute, Yokohama City University Graduate School of Medicine, Yokohama, Japan. [5]Departments of Gynecologic Oncology and Cancer Biology, Center for RNA Interference and Non-Coding RNA, University of Texas M.D. Anderson Cancer Center, Houston, Texas, USA.

Chronic pain is a major clinical problem, yet the mechanisms underlying the transition from acute to chronic pain remain poorly understood. In mice, reduced expression of GPCR kinase 2 (GRK2) in nociceptors promotes cAMP signaling to the guanine nucleotide exchange factor EPAC1 and prolongs the PGE_2-induced increase in pain sensitivity (hyperalgesia). Here we hypothesized that reduction of GRK2 or increased EPAC1 in dorsal root ganglion (DRG) neurons would promote the transition to chronic pain. We used 2 mouse models of hyperalgesic priming in which the transition from acute to chronic PGE_2-induced hyperalgesia occurs. Hyperalgesic priming with carrageenan induced a sustained decrease in nociceptor GRK2, whereas priming with the PKCε agonist ΨεRACK increased DRG EPAC1. When either GRK2 was increased in vivo by viral-based gene transfer or EPAC1 was decreased in vivo, as was the case for mice heterozygous for *Epac1* or mice treated with *Epac1* antisense oligodeoxynucleotides, chronic PGE_2-induced hyperalgesia development was prevented in the 2 priming models. Using the CFA model of chronic inflammatory pain, we found that increasing GRK2 or decreasing EPAC1 inhibited chronic hyperalgesia. Our data suggest that therapies targeted at balancing nociceptor GRK2 and EPAC1 levels have promise for the prevention and treatment of chronic pain.

Introduction

According to a recent report by the NIH, chronic pain affects more than 100 million people in the United States (1). The same report concludes that increased understanding of the mechanisms contributing to the development of chronic pain is key to finding novel interventions by which to prevent it.

Inflammatory mediators induce pain by direct activation of nociceptive terminals, but also increase the sensitivity to painful stimuli, a phenomenon known as hyperalgesia (2–4). This inflammatory hyperalgesia is generated by peripheral sensitization of nociceptive neurons as well as by central sensitization at the level of the spinal cord (5–7). In most cases, inflammatory pain and hyperalgesia resolve after resolution of inflammation or after tissues heal. However, in a significant subset of patients, pain does not resolve, and chronic pain develops. For example, approximately 10%–15% of patients with herpes zoster–induced rash develop postherpetic pain, defined as pain lasting at least 3 months after healing of the rash (8). Chronic postsurgical pain is observed even more frequently, for example, in patients undergoing thoracotomy (50%), breast surgery (30%), or cholecystectomy (10%–20%) (9).

The mechanisms underlying the development of persistent pain are poorly understood, and this is a major limitation for identification of new and adequate treatments. At the level of signaling pathways in peripheral nociceptors, recent studies have shown that mammalian target of rapamycin– (mTOR-) and ERK-dependent pathways play a critical role in chronic pain (10–14). Models of hyperalgesic priming have been developed as a tool to study the transition to chronic pain (10, 15, 16). In these models, short-lasting hyperalgesia is induced by intraplantar injection of, for example, a low dose of carrageenan, the PKCε activator ΨεRACK (HDAPIGYD; pseudoreceptor octapeptide for activated PKCε), or the inflammatory cytokine IL-6 into the hind paw (10, 15, 16). After this transient period of hyperalgesia, changes occur in primary sensory neurons that lead to marked prolongation of the hyperalgesic response to a subsequent exposure to the inflammatory mediator PGE_2 (10, 15–17). Both mTOR- and ERK-dependent pathways play a critical role in nociceptive plasticity in hyperalgesic priming (10). In addition, in rats primed with carrageenan or ΨεRACK, prolonged PGE_2-induced hyperalgesia depends on activation of ERK and PKCε. In naive rats, the classic cAMP/PKA pathway is critical for the transient hyperalgesia in response to PGE_2 (17). cAMP-to-PKCε signaling is thought to be mediated via exchange protein directly activated by cAMP (EPAC; refs. 18, 19), and EPAC activation by intraplantar injection of the specific agonist 8-pCPT-2′-O-Me-cAMP (8-pCPT) induces hyperalgesia via a PKCε-dependent route (20).

We identified nociceptor GPCR kinase 2 (GRK2) as a novel regulator of the duration of inflammatory hyperalgesia (21–27). GRK2 restrains signaling by promoting desensitization of GPCRs (28) and/or by interacting with multiple components of intracellular signaling pathways (22, 29, 30).

Using sensory neuron–specific *Grk2*-heterozygous mice (SNS-$Grk2^{+/-}$ mice), which have a cell-specific approximately 50% decrease in nociceptor GRK2, we previously showed that mechanical hyperalgesia induced by PGE_2 and other cAMP-inducing agents was significantly prolonged in mice with low nociceptor GRK2 (22, 25). Inhibition of PKA did not affect PGE_2 hyperalgesia in SNS-$Grk2^{+/-}$

Conflict of interest: The authors have declared that no conflict of interest exists.
Citation for this article: *J Clin Invest.* 2013;123(12):5023–5034. doi:10.1172/JCI66241.

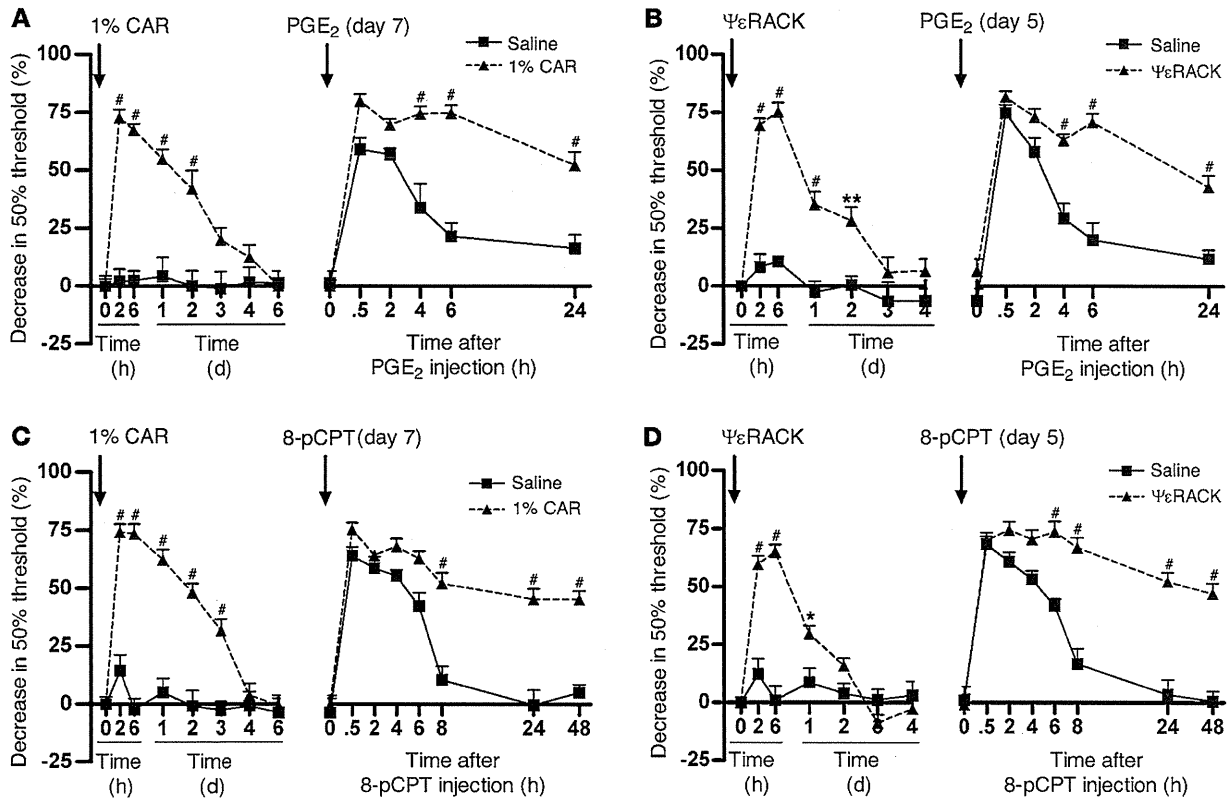

Figure 1

Hyperalgesic priming in mice. (**A** and **C**) 7 days after intraplantar carrageenan (CAR; 1%, 5 μl) or saline pretreatment or (**B** and **D**) 5 days after intraplantar ΨεRACK (1 μg/paw) or saline pretreatment, mice received an intraplantar injection of (**A** and **B**) PGE_2 (100 ng/paw) or (**C** and **D**) 8-pCPT (12.5 ng/paw). Changes in 50% paw withdrawal threshold were monitored over time. Data represent mean ± SEM. $n = 8$ per group. $^*P < 0.05$, $^{**}P < 0.01$, $^{\#}P < 0.001$.

mice, whereas inhibition of PKCε or ERK prevented the prolongation of PGE_2 hyperalgesia (22, 25). These findings indicate that the prolongation of PGE_2 hyperalgesia in GRK2-deficient mice involves activation of PKCε- and ERK-dependent signaling pathways (17, 22, 25). We also showed that GRK2 interacts with EPAC1 and inhibits its EPAC signaling to its downstream target, RAP1 (22). Moreover, chronic inflammatory pain is associated with a decrease in GRK2 in nociceptors (25). In addition, Ferrari and coworkers showed that a transient decrease in GRK2 resulting from treating rats intrathecally with *Grk2* antisense oligodeoxynucleotides (asODNs) prolonged hyperalgesia, in this case via a PKCε-independent and PKA- and SRC tyrosine kinase–dependent mechanism (31).

Here we tested the hypothesis that protein levels of GRK2 and EPAC1 in nociceptors represent key factors regulating persistent hyperalgesia. Using 2 mouse models of hyperalgesic priming, prior nociceptive sensitization with carrageenan and with ΨεRACK, we showed that the induced transition to chronic PGE_2 hyperalgesia was mediated by decreased GRK2 and increased EPAC1, respectively. We also showed that the prolongation of PGE_2 hyperalgesia in primed mice was inhibited by either upregulation of GRK2 or downregulation of EPAC1 after development of the primed state. These effects occurred regardless of whether GRK2 was decreased or EPAC1 was increased. Changing the balance between GRK2 and EPAC1 may have more general relevance for hyperalgesia, as we also showed using the CFA model of chronic inflammatory pain, in which increasing GRK2 or downregulating EPAC1 inhibited persistent mechanical hyperalgesia.

Results

Hyperalgesic priming. Hyperalgesic priming was induced in mice with an intraplantar injection of carrageenan or ΨεRACK. At 7 days after carrageenan and 5 days after ΨεRACK injection, primed mice received an intraplantar injection of PGE_2 or the EPAC activator 8-pCPT.

In carrageenan-primed mice, PGE_2-induced mechanical hyperalgesia lasted more than 24 hours, whereas in saline-treated mice, PGE_2 hyperalgesia resolved within 6 hours (Figure 1A). In ΨεRACK-primed mice, PGE_2 hyperalgesia was also prolonged to more than 24 hours (Figure 1B). Moreover, hyperalgesia induced by 8-pCPT exceeded 48 hours in carrageenan- and ΨεRACK-primed mice, compared with less than 8 hours in control mice (Figure 1, C and D).

Carrageenan priming also prolonged hyperalgesia induced by the cAMP-inducing mediator epinephrine from 4 days in control mice to almost 2 weeks in primed mice (Supplemental Figure 1A; supplemental material available online with this article; doi:10.1172/JCI66241DS1). Interestingly, carrageenan priming did not affect hyperalgesia induced by IL-1β (Supplemental Figure 1B), a proinflammatory mediator that does not induce cAMP signaling, but promotes hyperalgesia via a p38-mediated pathway.

GRK2 levels in primary sensory neurons of primed mice. We next determined whether hyperalgesic priming by carrageenan

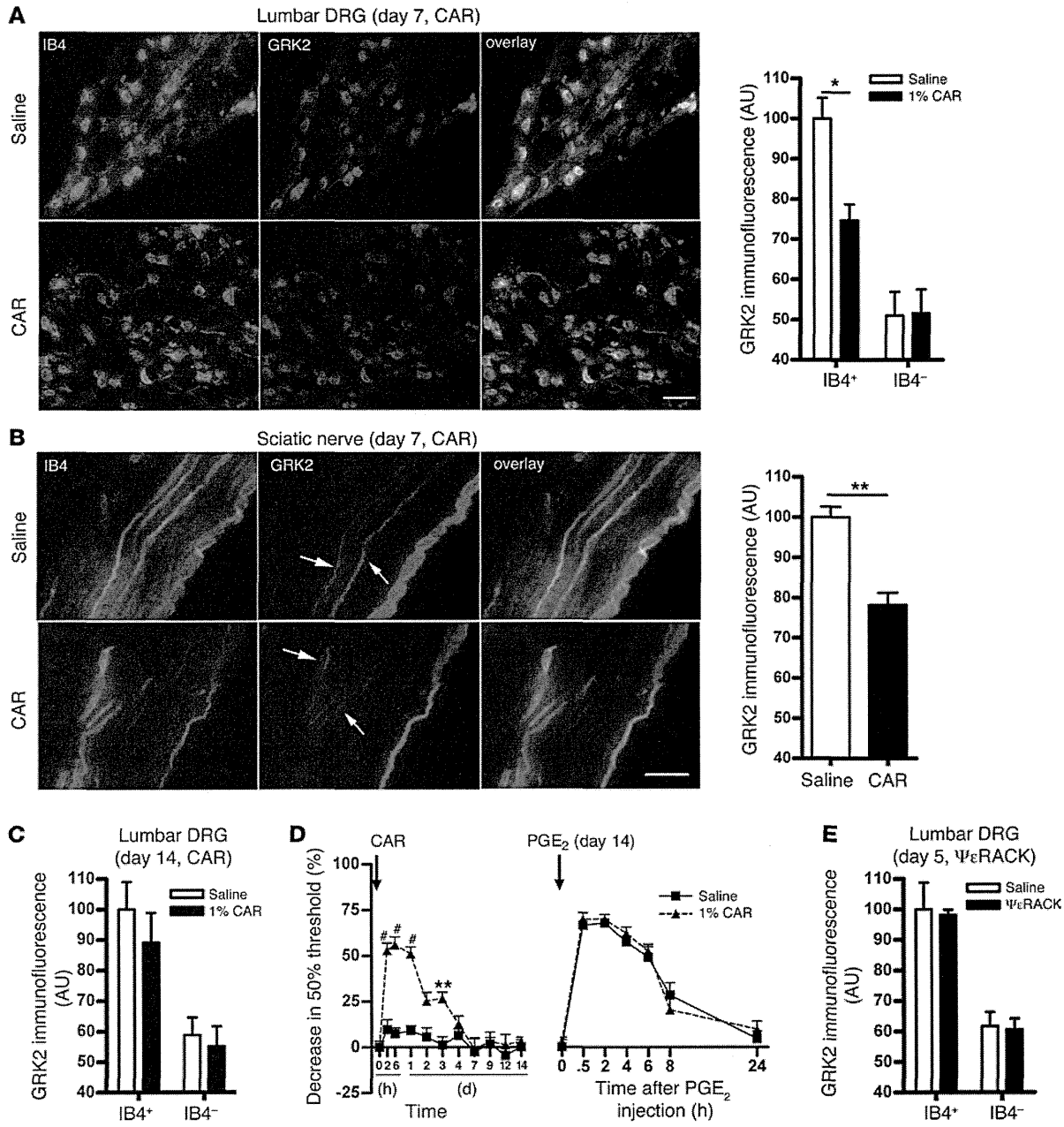

Figure 2

Carrageenan- and ΨεRACK-induced changes in sensory neuron GRK2 protein expression. (**A** and **B**) Mice received an intraplantar injection of 1% carrageenan or saline, and 7 days later, GRK2 protein levels in IB4$^+$ and IB4$^-$ neurons from lumbar DRG, thoracic DRG, and sciatic nerve fibers were quantified by immunofluorescence analysis. Shown are representative images of IB4 (green) and GRK2 (red) double staining of (**A**) lumbar DRG and (**B**) sciatic nerves, and mean GRK2 immunofluorescence intensity in (**A**) lumbar or thoracic DRG and (**B**) sciatic nerve fibers. Scale bars: 50 μm. (**C**) Mean GRK2 immunofluorescence intensity in lumbar DRG at 14 days after intraplantar carrageenan or saline. (**D**) 14 days after carrageenan or saline pretreatment, mice received an intraplantar injection of PGE_2 (100 ng/paw). Changes in 50% paw withdrawal threshold were monitored over time. (**E**) Mean GRK2 immunofluorescence intensity in lumbar DRG at 5 days after intraplantar ΨεRACK or saline. Data represent mean ± SEM (n = 4 per group), based on approximately 300 neurons from lumbar DRG per mouse. $^*P < 0.05$, $^{**}P < 0.01$, $^{\#}P < 0.001$.

decreases neuronal GRK2 protein levels in dorsal root ganglion (DRG) and sciatic nerve. Because the isolectin B4–positive (IB4$^+$) subpopulation of DRG neurons is known to be involved in hyperalgesic priming (32, 33), we used IB4 as a marker to identify this specific subgroup of sensory neurons.

At 3 and 7 days after intraplantar carrageenan injection into the hind paws, the level of GRK2 in small-diameter IB4$^+$ neurons was reduced by approximately 25% in lumbar DRG (Figure 2A and Supplemental Figure 2). There was no change in GRK2 protein levels in small-diameter IB4$^-$ neurons in lumbar DRG after

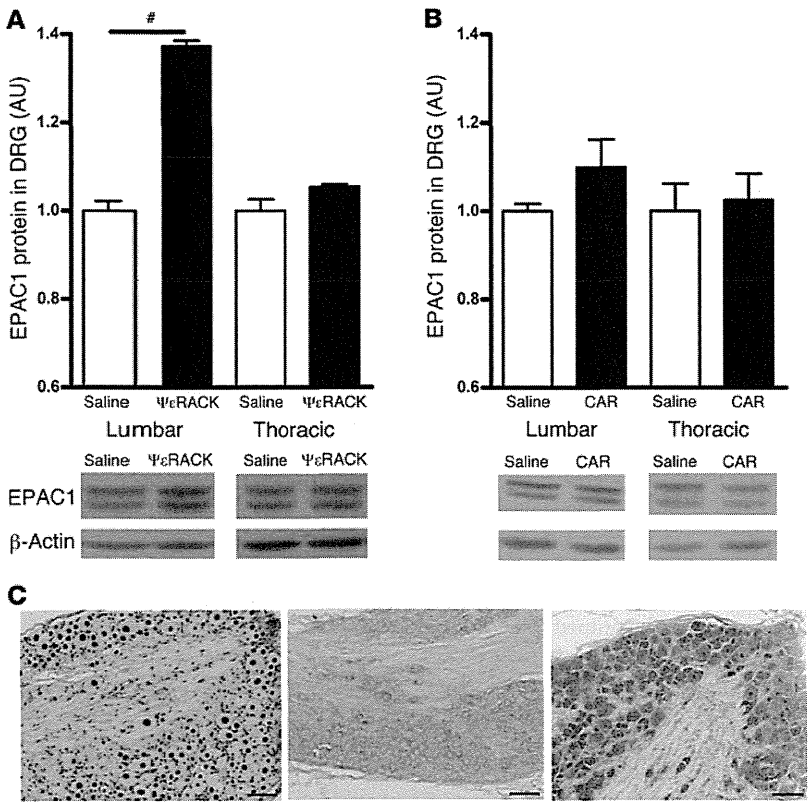

Figure 3
EPAC1 level in DRG after carrageenan- and ΨεRACK-induced priming. (**A** and **B**) EPAC1 protein level in DRG, determined by Western blot analysis of DRG tissue homogenates, at (**A**) 5 days after ΨεRACK priming and (**B**) 7 days after carrageenan priming. Data represent mean ± SEM (n = 4 per group). $^{\#}P < 0.001$. (**C**) Cellular distribution of *Epac1* mRNA expression was analyzed by in situ hybridization analysis of lumbar DRG from untreated mice. Representative example from 1 mouse of 3 with similar results. Left: Nuclear staining of positive control (U6 small nuclear RNA probe). Middle: Negative control probe. Right: *Epac1* probe. Scale bars: 20 μm.

carrageenan priming (Figure 2A and Supplemental Figure 2). In addition, GRK2 levels did not change in thoracic DRG neurons at any time point (Supplemental Figure 3). Western blot analysis of DRG homogenates did not detect changes in GRK2 protein at day 7 after carrageenan priming (Supplemental Figure 4). This is likely due to reduced GRK2 only in IB4$^+$ sensory neurons in response to intraplantar carrageenan.

The carrageenan-induced GRK2 decrease in the soma of IB4$^+$ sensory neurons was also reflected in a decrease in axonal GRK2; at 7 days after carrageenan injection, the level of GRK2 in IB4$^+$ fibers was reduced by approximately 20% in the carrageenan- versus the saline-pretreated group (Figure 2B).

At day 14 after intraplantar carrageenan injection, GRK2 levels in small-diameter IB4$^+$ sensory neurons had returned to baseline levels (Figure 2C). The primed state had also resolved at 14 days after carrageenan injection; the course of PGE_2 hyperalgesia did not differ between the saline- and carrageenan-pretreated groups at this time point (Figure 2D). These findings show that resolution of the primed state is associated with normalization of GRK2 protein levels.

Notably, when we evaluated GRK2 levels in lumbar DRG at 5 days after ΨεRACK priming, we did not observe any change in GRK2 level. The levels of GRK2 were similar in small-diameter IB4$^+$ lumbar sensory neurons from ΨεRACK-primed and saline-treated mice (Figure 2E). Furthermore, no changes in GRK2 levels were observed in IB4$^-$ lumbar DRG neurons or in thoracic DRG neurons after ΨεRACK priming (Supplemental Figure 3).

EPAC1 level in DRG after carrageenan and ΨεRACK priming. After both carrageenan and ΨεRACK priming, hyperalgesia induced by 8-pCPT was significantly prolonged. These findings indicate that in both cases, the primed state is associated with a prolonged hyperalgesic response to EPAC activation. We hypothesized that either a decrease in GRK2 or an increase in EPAC1 would be sufficient to facilitate EPAC1-mediated signaling leading to prolonged PGE_2 hyperalgesia. To test this hypothesis, we measured the level of EPAC1 in DRG in these 2 priming conditions. The antibodies available for EPAC1 did not allow reliable staining for this protein in sensory neurons. Therefore, we analyzed EPAC1 levels by Western blotting. EPAC1 levels in lumbar DRG of ΨεRACK-primed mice were increased by approximately 35% compared with levels in saline-treated mice, whereas carrageenan priming did not induce a detectable change in EPAC1 (Figure 3, A and B). To determine which cells in the DRG express EPAC1, we used an in situ hybridization approach. Virtually all neurons in the DRG stained positively for *Epac1* mRNA (Figure 3C).

Effect of GRK2 gene transfer on treatment of hyperalgesic priming. To determine whether the observed changes in GRK2 and EPAC1 levels in the DRG represent potential targets for the prevention of chronic pain, we first examined the effect of increasing GRK2 in DRG neurons in vivo after hyperalgesic priming with carrageenan and ΨεRACK. We used a herpes simplex virus (HSV; ref. 34) vector encoding bovine *GRK2* and *GFP* as a reporter protein (referred to herein as HSV-*GRK2*) or a control HSV vector containing *GFP* only (HSV-*GFP*). In carrageenan-primed mice, treatment with 2.5 μl of 1.4×10^7 pfu/ml HSV-*GRK2* at days 3 and 5 significantly shortened PGE_2 hyperalgesia compared with mice treated with HSV-*GFP* (Figure 4A). In ΨεRACK-primed mice, HSV-*GRK2* also shortened PGE_2 hyperalgesia compared with mice treated with the same dose of HSV-*GFP* (Figure 4B). This effect of *GRK2* overexpression occurred even though ΨεRACK priming did not induce a detectable decrease in GRK2 protein in DRG neurons (Figure 2E).

PGE_2 hyperalgesia lasted about 8 hours in both HSV-*GRK2*– and HSV-*GFP*–treated mice that had not been exposed to carrageenan or ΨεRACK (Figure 4C), which indicates that in naive mice, *GRK2* overexpression in sensory neurons does not affect the pain response.

Inoculation with HSV induced a transient and small increase in mechanical sensitivity that resolved within 1–2 days and was independent of the presence of *GRK2* (Figure 4, A–C). Therefore, it is unlikely that this acute response to the virus contributed to the observed inhibition of the primed phenotype.

To confirm successful *GRK2* gene transfer, we analyzed expression of the *GFP* reporter in lumbar DRG, sciatic nerve, and skin of the injected paw 3 days after the last HSV injection. GFP

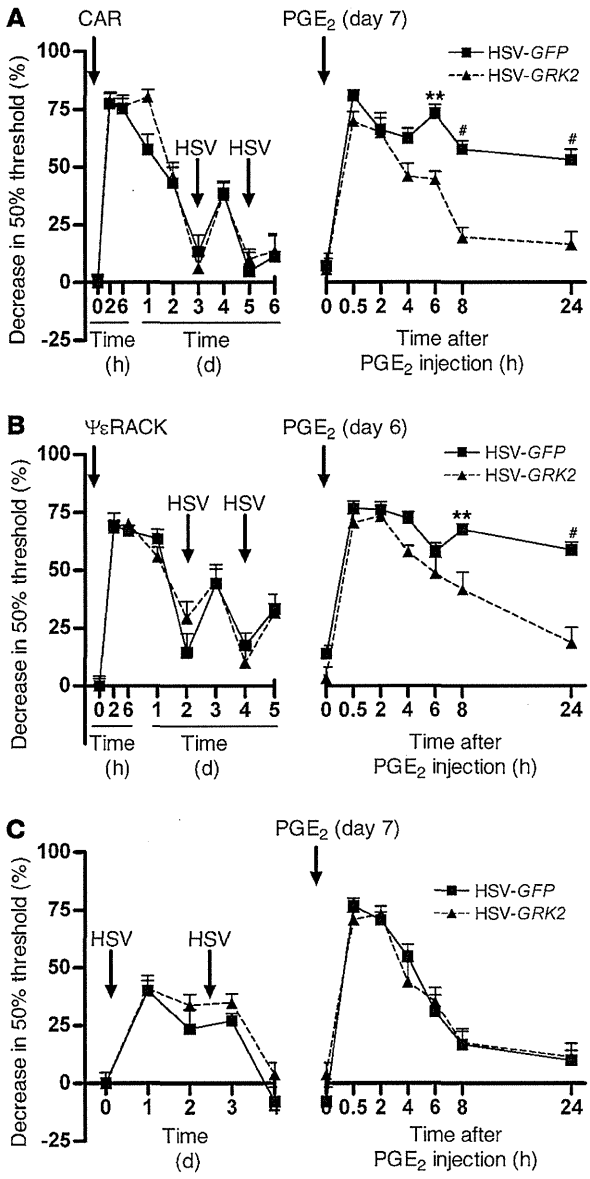

Figure 4
Effect of HSV-mediated GRK2 overexpression on carrageenan- and ΨεRACK-induced hyperalgesic priming. (**A**) Carrageenan-primed, (**B**) ΨεRACK-primed, or (**C**) naive control mice were inoculated intraplantarly with 2 injections of HSV-*GRK2* or HSV-*GFP* (1.4×10^7 pfu/ml, 2.5 μl/paw) followed by PGE_2 (100 ng/paw). Changes in 50% paw withdrawal threshold were monitored over time. Data represent mean ± SEM ($n = 8$ per group). $^{**}P < 0.01$, $^{\#}P < 0.001$.

expression was clearly visible in both IB4$^+$ and IB4$^-$ small-diameter DRG neurons and in both IB4$^+$ and IB4$^-$ fibers in the sciatic nerve (Figure 5, A–F). GFP was also detected in peripherin$^+$ nerves in the skin (Figure 5, G–I).

Next, we determined whether GRK2 kinase activity is required to prevent transition to chronic pain after priming, using an HSV construct expressing *GRK2*^{K220R}, the kinase-dead mutant of *GRK2* (35). *GRK2*^{K220R} did not reverse the primed state (Figure 6). The course of PGE_2 hyperalgesia in primed mice treated with HSV-*GRK2*^{K220R} was similar to that of primed mice receiving control HSV-*GFP* inoculation.

Collectively, our data indicate that, independently of whether priming decreased GRK2 or increased EPAC1 expression, HSV-mediated *GRK2* overexpression was sufficient to reverse the primed state, thereby preventing the development of persistent hyperalgesia.

Hyperalgesic priming in Epac1$^{+/-}$ *mice.* To further test our hypothesis that the GRK2/EPAC1 system regulates the transition to chronic hyperalgesia in primed mice, we used mice with heterozygous knockout of *Epac1* (*Epac1*$^{+/-}$ mice; ref. 36). These mice had an approximately 50% reduction in EPAC1 protein in the DRG (Figure 7A). In response to carrageenan and ΨεRACK priming, *Epac1*$^{+/-}$ mice did not show the prolongation of PGE_2 hyperalgesia observed in WT mice (Figure 7, B and C). The course of PGE_2 hyperalgesia did not differ between *Epac1*$^{+/-}$ and WT mice that were not primed (Figure 7D).

Effect of intrathecal Epac1 asODNs on hyperalgesic priming. The results we obtained in *Epac1*$^{+/-}$ mice suggested that hyperalgesic priming can be prevented by lowering EPAC1 levels. We next tested whether the primed state can also be treated by temporarily downregulating EPAC1 protein levels in sensory neurons using intrathecal injection of *Epac1* asODNs. *Epac1* asODN treatment significantly reduced the duration of PGE_2 hyperalgesia in mice primed with carrageenan or ΨεRACK (Figure 8, A and C). In lumbar DRG, protein levels of EPAC1 in carrageenan- and ΨεRACK-primed mice decreased significantly after intrathecal *Epac1* asODN injection (Figure 8, B and D).

The *Epac1* asODN–mediated decrease in EPAC1 protein levels did not change the baseline mechanical pain threshold or the duration and severity of acute PGE_2 hyperalgesia in naive mice (Figure 8, E and F). Intrathecal administration of *Epac1* asODNs did not affect the protein levels of EPAC2 (Supplemental Figure 5).

Effect of HSV-GRK2 or intrathecal Epac1 asODN in a model of chronic inflammatory pain. To determine the broader relevance of the GRK2/EPAC1 system for chronic pain, we used the CFA model of chronic inflammatory pain. HSV-*GRK2* treatment significantly attenuated the chronic mechanical hyperalgesia that developed in response to CFA (Figure 9A). Intrathecal administration of *Epac1* asODNs also reduced the chronic CFA-induced mechanical hyperalgesia (Figure 9B). In CFA-treated mice, GRK2 levels in IB4$^+$ DRG neurons were decreased at day 5 after CFA injection (Figure 9C). We did not detect changes in GRK2 protein by Western blot analysis (Supplemental Figure 6). Consistent with earlier studies (37), DRG EPAC1 levels were increased in CFA-treated mice (Figure 9D).

Discussion

Although it is widely accepted that acute and chronic pain are different entities that depend on specific neurobiological pathways, knowledge about the underlying mechanisms remains limited. Here, we uncovered 2 key regulators of the development and maintenance of persistent pain in response to repeat or chronic inflammation: the kinase GRK2, and the cAMP sensor EPAC1. Specifically, using carrageenan and ΨεRACK priming as mouse models of the transition to persistent hyperalgesia, we showed that the prolongation of the hyperalgesic response in primed mice is associated with a sustained decrease in GRK2 level or increase in EPAC1 level in DRG (Figure 10). The functional importance of this observation is attested by our findings that increasing nociceptor GRK2 or decreasing EPAC1 prevented per-

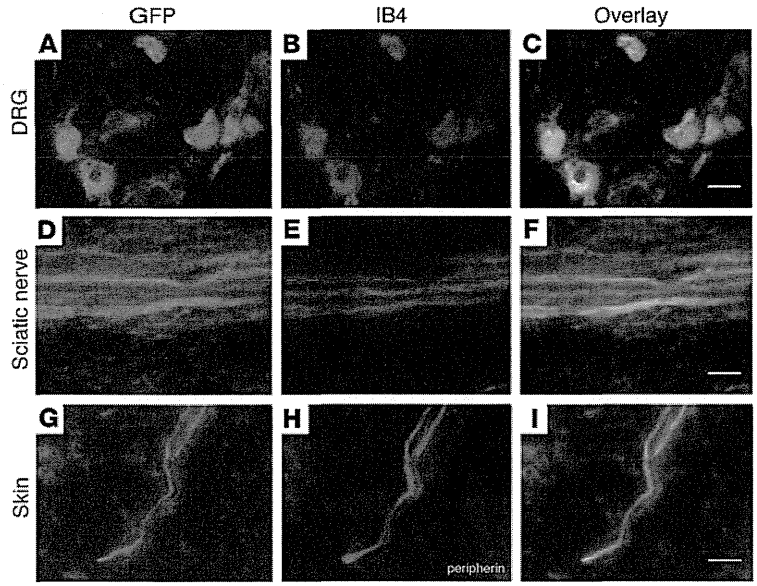

Figure 5
HSV-mediated overexpression of *GRK2* and *GFP*. Expression of GFP (**A**, **D**, and **G**), an indicator of successful transgene expression, was observed in IB4$^+$ lumbar DRG neurons (**B**), IB4$^+$ sciatic nerve fibers (**E**), and peripherin$^+$ nerve endings (**H**) in the skin at 2 days after the last inoculation with HSV-*GRK2* in primed mice. (**C**, **F**, and **I**) Merged images showing overlay. Scale bars: 20 μm.

sistent hyperalgesia in primed mice. Notably, increasing GRK2 expression prevented the prolongation of PGE_2 hyperalgesia in primed mice, regardless of whether GRK2 was decreased (after carrageenan priming) or EPAC1 was increased (after ΨεRACK priming). Similarly, downregulating EPAC1 inhibited the primed phenotype when GRK2 was decreased without a change in EPAC1 (in the carrageenan model), as well as when GRK2 was unchanged and EPAC1 was increased (in the ΨεRACK model). On the basis of these novel findings, we propose that an imbalance between the protein levels of GRK2 and EPAC1 is sufficient to cause the prolongation of hyperalgesia in primed mice. We also propose that reestablishing the GRK2/EPAC1 balance can be considered as a novel avenue for the prevention of persistent pain.

Importantly, the role of GRK2 and EPAC1 is not restricted to persistent hyperalgesia in priming models. In the well-established model of CFA-induced chronic inflammatory pain, DRG GRK2 was increased and EPAC1 decreased. Moreover, increasing GRK2 or decreasing EPAC1 during ongoing inflammatory pain inhibited chronic CFA-induced hyperalgesia. This is important because it indicates that targeting GRK2/EPAC1 may both prevent chronic pain and combat existing chronic pain, such as that experienced by patients with painful inflammatory diseases like arthritis.

We confirmed earlier findings that DRG EPAC1 levels are increased in the CFA model of chronic inflammatory pain (37). In addition, we showed that the CFA model was associated with reduced GRK2 in IB4$^+$ nociceptors. Interestingly, the mechanical hyperalgesia that develops in the CFA model was inhibited by increasing nociceptor GRK2 or by decreasing EPAC1 levels. DRG EPAC1 levels are also increased in the L5 spinal nerve transection model of chronic neuropathic pain in mice (38). In addition, nerve damage–induced mechanical hyperalgesia was significantly reduced in *Epac1*$^{+/-}$ and *Epac1*$^{-/-}$ mice (38). In vitro, EPAC1 signaling enhances Piezo2-mediated mechanotransduction in sensory neurons (38). Our findings demonstrated that EPAC1 is also a key to promoting mechanical hyperalgesia in primed mice as well as in a classic model of chronic inflammatory pain. Moreover, our findings indicate that decreased nociceptor GRK2 promotes persistent hyperalgesia in a priming model and contributes to chronic inflammatory pain. It remains to be determined whether HSV-*GRK2*–mediated overexpression of GRK2 also attenuates chronic neuropathic pain.

In naive animals, cAMP-inducing agents such as PGE_2 and epinephrine induce hyperalgesia via the classic cAMP target PKA (17, 22, 25). However, in primed rats or in mice with genetically low

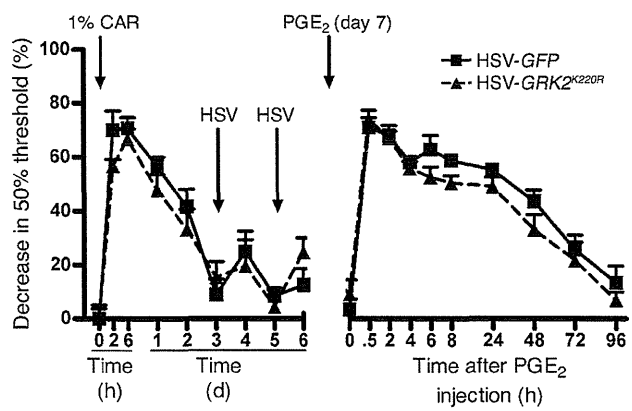

Figure 6
Effect of overexpression of the *GRK2* kinase-dead mutant, *GRK2*^{K220R}, on carrageenan-induced hyperalgesic priming. Carrageenan-primed mice were inoculated intraplantarly with 2 injections of HSV-*GRK2*^{K220R} or HSV-*GFP* followed by PGE_2 (100 ng/paw). Changes in 50% paw withdrawal threshold were monitored over time. Data represent mean ± SEM (n = 8 per group).

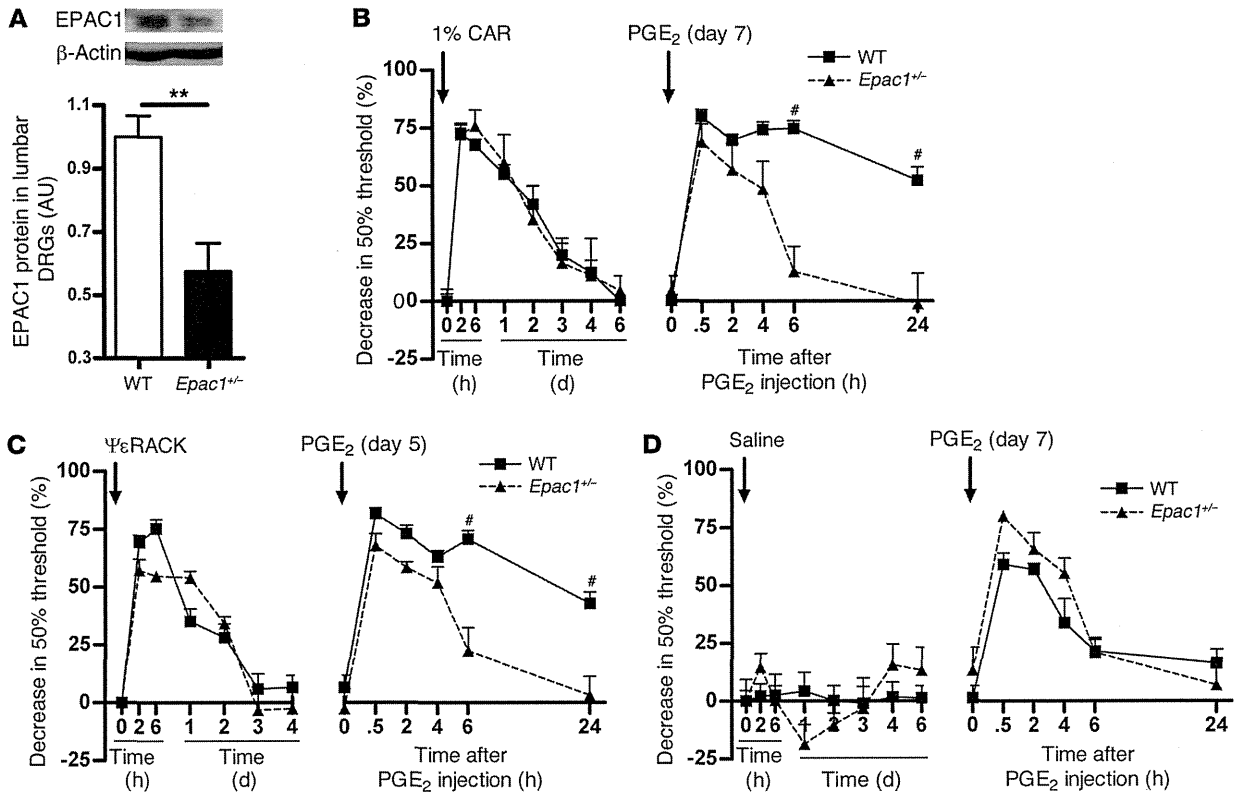

Figure 7

Hyperalgesic priming in *Epac1*$^{+/-}$ mice. (**A**) EPAC1 protein level, determined by Western blot analysis of DRG tissue homogenates from WT and *Epac1*$^{+/-}$ mice (n = 4 per group). (**B**) 7 days after carrageenan pretreatment (n = 4 per group), (**C**) 5 days after intraplantar ΨεRACK pretreatment (1 μg/paw in 5 μl saline; n = 6 per group), or (**D**) 7 days after saline pretreatment (n = 4 per group), mice received an intraplantar injection of PGE_2 (100 ng/paw in 2.5 μl saline). Changes in 50% paw withdrawal threshold were monitored over time. Data represent mean ± SEM. $^{**}P < 0.01$, $^{\#}P < 0.001$.

levels of nociceptor GRK2, inhibition of PKA does not inhibit hyperalgesia induced by these agents. In primed rats or nociceptor GRK2–deficient mice, inhibition of PKCε or ERK prevents prolongation of 8-Br-cAMP, PGE_2, or epinephrine hyperalgesia. These findings indicate that priming and *Grk2* deficiency both promote ERK- and PKCε-mediated hyperalgesic signaling in response to cAMP-inducing agents (17, 22, 25). Levine and colleagues were the first to show that activation of the alternative cAMP sensor EPAC induces hyperalgesia via a PKCε-mediated pathway (20). Hyperalgesia induced by 8-pCPT is also prolonged in conditions of SNS-*Grk2* deficiency (22). Moreover, in vitro, low GRK2 promotes 8-pCPT signaling to the EPAC target RAP1 and to ERK (22). On the basis of these earlier in vitro findings and our present in vivo findings, we hypothesize that the shift in the balance between GRK2 and EPAC1 levels in the DRG in primed mice and in mice with chronic inflammatory pain may promote EPAC1 signaling and persistent mechanical hyperalgesia. Consistently, hyperalgesia induced by 8-pCPT was prolonged after priming with carrageenan as well as ΨεRACK. Treatment of primed mice with HSV-*GRK2*^{K220R} did not reverse the primed state, which indicates that GRK2 kinase activity is required for inhibiting pain signaling. Future studies should investigate whether GRK2 directly phosphorylates EPAC1 to inhibit EPAC1 activation and control the pain response.

Earlier studies have shown that activation of the mTOR pathway and protein translation in the periphery are required for development of IL-6– and carrageenan-induced priming of the subsequent response to PGE_2 (10, 11, 17, 39). Axonal protein synthesis under the control of mTOR and ERK activation contribute to chronic pain in multiple other models as well (12–14). ERK activation also contributes to the prolonged PGE_2 hyperalgesia in *Grk2*-deficient mice, and ERK activation by 8-pCPT is increased in *Grk2*-deficient cells (22). Notably, stimulation of prostate cancer cells with 8-pCPT activates the mTOR pathway (40, 41). Thus, it is conceivable that increased EPAC signaling promotes persistent pain via downstream activation of ERK and mTOR signaling pathways, leading to peripheral protein translation.

GRK2 protein is reduced in peripheral blood lymphocytes from humans with rheumatoid arthritis or multiple sclerosis (42, 43) and in splenocytes from rats with adjuvant arthritis or EAE (44, 45). In all these examples, the reduction in GRK2 was not associated with a change in *Grk2* mRNA, which indicates that regulation takes place at the posttranslational level. The inflammation in rats with adjuvant arthritis spontaneously resolves approximately 30 days after induction. However, GRK2 levels in splenocytes were still reduced by 50% 2 weeks after resolution of inflammation (44). Similarly, we showed here that GRK2 levels in DRG neurons remained decreased even after resolution of the inflammation-

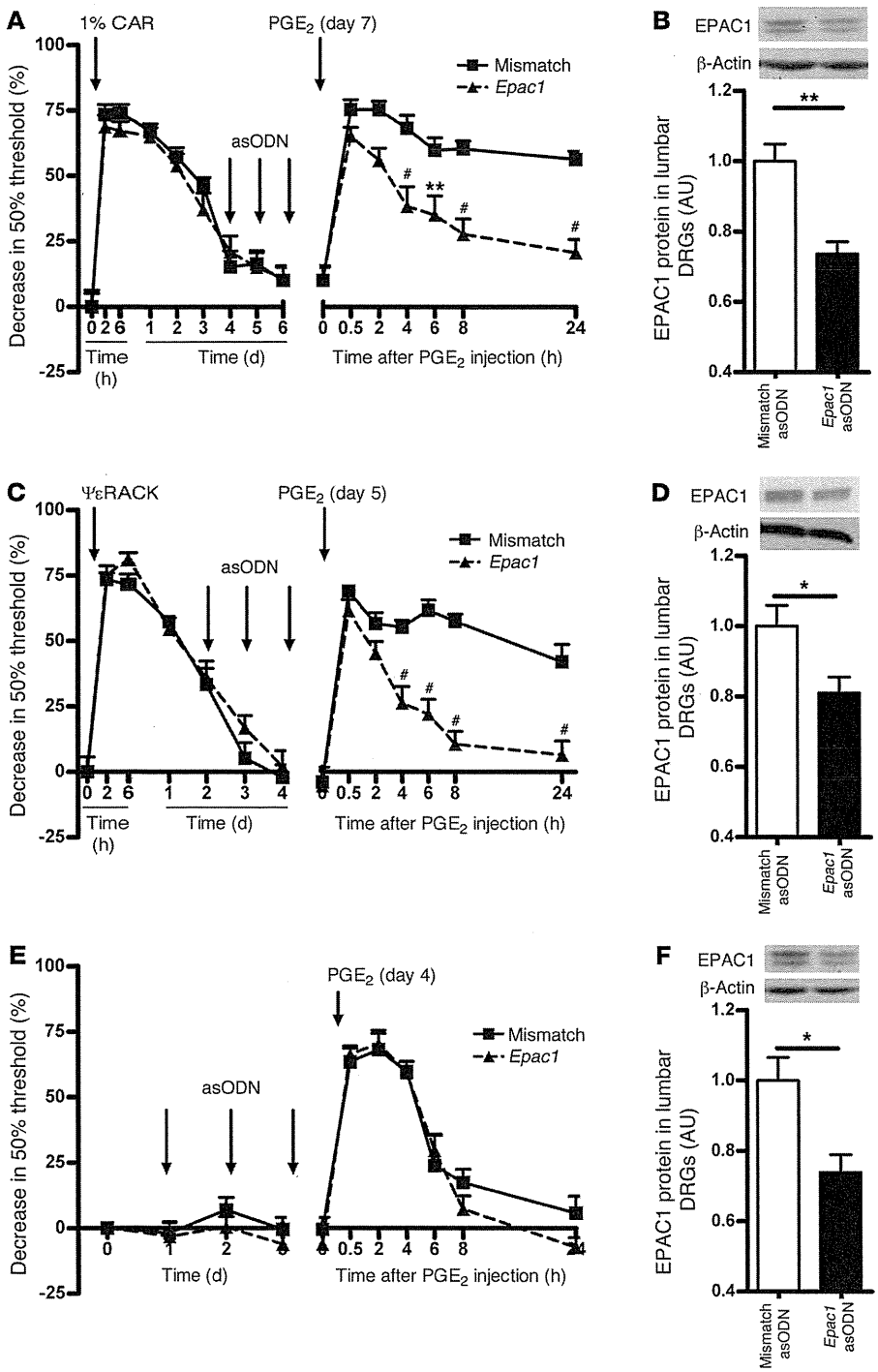

Figure 8
Effect of intrathecal *Epac1* asODNs on carrageenan- and ΨεRACK-induced hyperalgesic priming. 3 days before intraplantar PGE_2 injection (100 ng/paw, in 2.5 μl saline), mice primed with (**A** and **B**) carrageenan or (**C** and **D**) ΨεRACK or (**E** and **F**) naive mice received 3 daily intrathecal injections of *Epac1* or mismatch control asODNs. (**A**, **C**, and **E**) Changes in 50% paw withdrawal threshold were monitored over time (n = 8 per group). (**B**, **D**, and **F**) EPAC1 levels were determined by Western blot 2 days after the last asODN treatment (n = 4 per group). Data represent mean ± SEM. $^*P < 0.05$, $^{**}P < 0.01$, $^{\#}P < 0.001$.

induced hyperalgesia. Very little is known about regulation of the cellular level of EPAC1, and it remains to be determined via which mechanism the amount of GRK2 protein is kept at a lower level in $IB4^+$ nociceptors or the DRG EPAC1 content is maintained at a higher level during the primed state.

Both in the carrageenan model of hyperalgesic priming and in the CFA model of chronic inflammatory pain, the reduction in GRK2 expression was restricted to small-diameter $IB4^+$ sensory neurons. It is well known that specific sets of sensory neurons are involved in different pain modalities and, more importantly, different types of chronic pain (46–49). The $IB4^+$ subset of DRG neurons specifically responds to inflammatory stimuli injected intraplantarly (46–49). Depletion of $IB4^+$ neurons completely ablates the primed phenotype, which indicates that priming induces changes with functional consequences specifically for $IB4^+$ neurons (32, 33). Moreover, selective changes occur in specific sets of neurons during inflammatory pain, including specific changes limited to $IB4^+$ neurons (33, 50, 51). It remains to be determined,

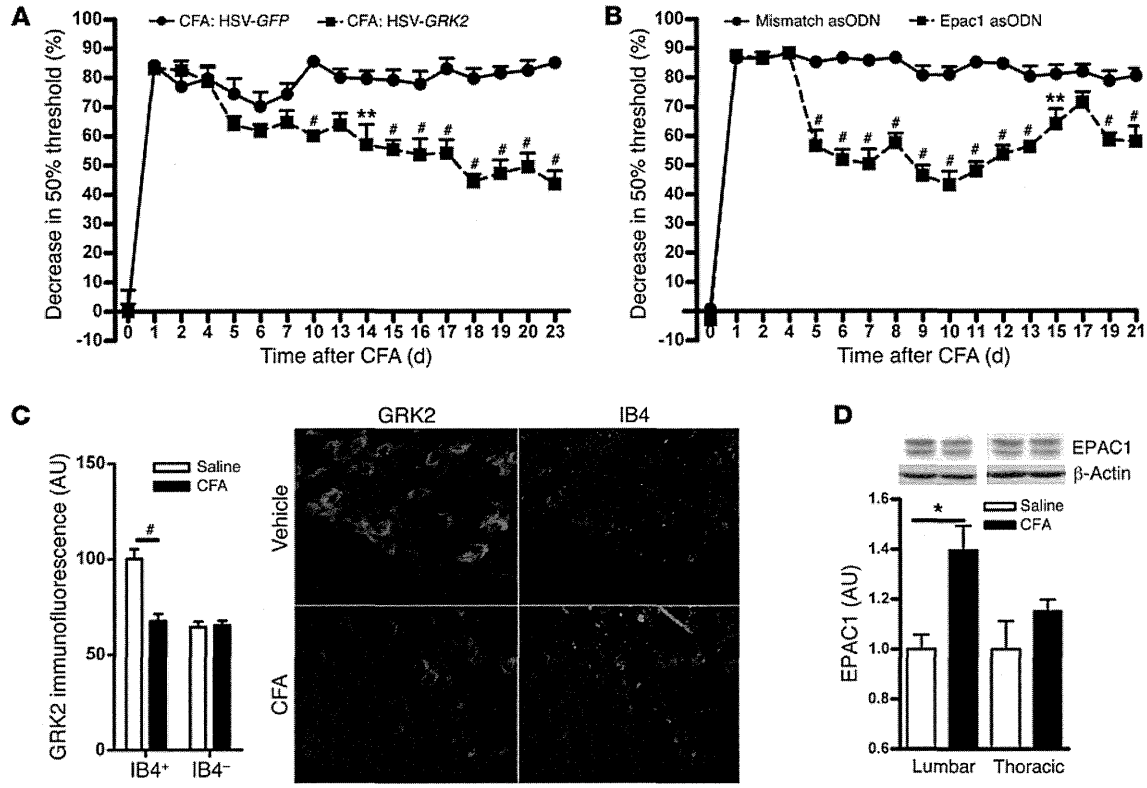

Figure 9

Effect of intraplantar HSV-*GRK2* or intrathecal *Epac1* asODNs on mechanical hyperalgesia in CFA-induced chronic inflammatory pain. (**A** and **B**) Mice were treated (**A**) intraplantarly with HSV-*GRK2* or HSV-*GFP* on days 4, 6, 13, and 16 after intraplantar CFA ($n = 6$ per group) or (**B**) intrathecally with *Epac1* or mismatch asODNs on days 4, 5, 6, 8, and 10 after intraplantar CFA ($n = 8$ per group). Changes in 50% paw withdrawal threshold were monitored over time. (**C**) Lumbar DRG were collected on day 5 after intraplantar CFA or saline, and GRK2 protein levels in DRG neurons were analyzed as described in Figure 1. Scale bar: 50 μm. (**D**) EPAC1 protein levels in lumbar DRG were quantified by Western blotting at day 5 after intraplantar saline or CFA ($n = 4$ per group). Data represent mean ± SEM. $^*P < 0.05$, $^{**}P < 0.01$, $^{\#}P < 0.001$.

however, which mechanisms govern the decrease in GRK2 specifically in IB4$^+$ small-diameter DRG neurons.

GRK2 was decreased in IB4$^+$ DRG neurons in the carrageenan model of hyperalgesic priming as well as in the CFA model of chronic inflammatory pain that depends on Nav1.8$^+$ nociceptors (52). After administration of HSV-*GRK2*, the GFP reporter protein was detected predominantly in IB4$^+$ small-diameter neurons and in IB4$^+$ nerve fibers in the sciatic nerve. This distribution of transgene expression after HSV-mediated gene transfer is consistent with earlier reports (53) and highlights HSV-mediated gene transfer as a specific tool by which to target small-diameter sensory neurons important in inflammatory pain processing. Nociceptor-specific targeting of GRK2 might prevent adverse effects in large-diameter neurons, likely leaving touch sensations unaffected (53). Indeed, mechanical sensitivity in naive mice, as determined using von Frey hairs, was unaffected by HSV-*GRK2*. Similarly, *Grk2*-deficient mice exhibit normal heat sensitivity under baseline conditions (21). Whether acute nociception of noxious stimuli such as mechanical pressure or heat is affected by changing EPAC1 levels remains to be determined.

HSV-*GRK2* treatment shortened PGE_2 hyperalgesia in primed mice and attenuated CFA-induced chronic hyperalgesia. These findings are consistent with our hypothesis that reduced GRK2 in IB4$^+$ nociceptors is a key factor that contributes to priming and to chronic inflammatory pain. Unfortunately, the available EPAC1 antibodies did not allow reliable quantification of EPAC1 expression in DRG neurons by immunohistochemistry, and therefore we do not know in which DRG neurons EPAC1 levels were increased after priming. However, in situ hybridization analysis demonstrated that *Epac1* mRNA was expressed in all cells in the DRG, including small-diameter neurons. We also showed that reducing DRG EPAC1 expression reversed the primed phenotype; this was the case even when DRG EPAC1 levels were not affected as GRK2 levels increased in small-diameter IB4$^+$ neurons. Notably, expression of GRK2 using the HSV-*GRK2* amplicon also inhibited the primed phenotype when GRK2 levels were not affected as EPAC1 levels were increased, for example, after ΨεRACK priming. Taken together, these findings support the hypothesis that a GRK2/EPAC1-dependent pathway in small-diameter nociceptors contributes to the primed phenotype. However, we cannot presently exclude that other, or additional, effects of changing GRK2 and EPAC1 levels in these and other cells ultimately are responsible for the observed inhibition of the primed phenotype when increasing GRK2 or decreasing EPAC1.

GRK2 and EPAC1 are widely expressed in both human and rodent tissues, including brain, heart, and thyroid gland, and

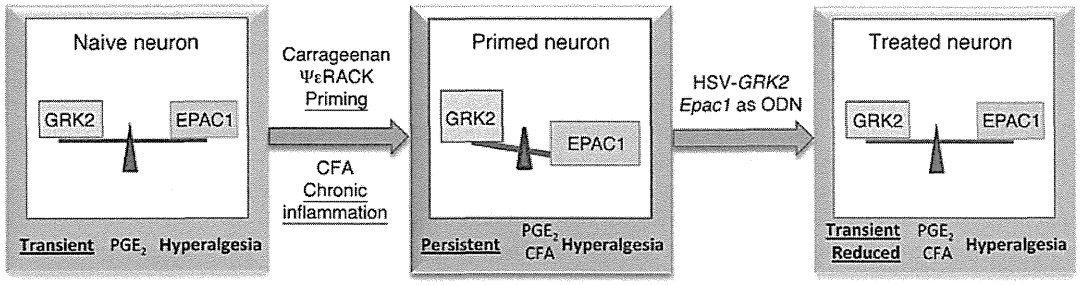

Figure 10
Schematic representation of our working model. Decreased GRK2 in peripheral sensory neurons and/or increased EPAC1 promotes the development of persistent hyperalgesia. Treatment with intraplantar HSV-*GRK2* or intrathecal *Epac1* asODNs normalizes the GRK2/EPAC1 balance, leading to inhibition of persistent hyperalgesia.

are likely to regulate a wide array of physiological processes (18, 19, 54–58). Therefore, changes in the protein levels of GRK2 and EPAC1 in other tissues may have important consequences for cAMP signaling and (patho)physiology. This potentially widespread importance of GRK2/EPAC1 makes it unlikely that systemic treatments aimed at increasing GRK2 or decreasing EPAC1 will be of therapeutic benefit. The approach we used here, in which we locally administered HSV amplicons to overexpress *GRK2* specifically in the area in which the increased pain response occurs, may be much more relevant. Another benefit of targeting the GRK2/EPAC system in sensory neurons is that by directly targeting intracellular signaling pathways involved in the transition to chronic pain, only the "pathological" transition to chronic pain is targeted, while evolutionary beneficial acute pain is not affected. Indeed, our data showed that increasing GRK2 in naive mice did not affect acute mechanical PGE_2 hyperalgesia. In addition, acute carrageenan and ΨεRACK priming–induced hyperalgesia was unaffected in *Epac1*$^{+/-}$ mice.

The important question arises as to whether the priming phenomenon occurs in humans. A recent experimental study in humans showed that pre-exposure to a mild inflammatory stimulus (low-dose endotoxin) increased the hyperalgesic response to subsequent intradermal injection of capsaicin (59). Clinically, there is evidence that repeat surgery for recurring inguinal hernia increases the risk of chronic postoperative pain (9, 60, 61). In addition, gastrointestinal infection is a risk factor for irritable bowel disorder, a condition in which, for example, ingestion of food can induce a pain response (62). These observations indicate that in humans, previous exposure to tissue damage and/or inflammation may also sensitize (prime) the pain response to subsequent challenge, reminiscent of hyperalgesic priming. Increasing EPAC1 or decreasing GRK2 prevented the development of persistent hyperalgesia in mice primed by transient local inflammation. Therefore, we propose that targeting GRK2/EPAC1 prior to repeat surgery or in patients with irritable bowel disorder may help prevent or treat persistent pain in these situations that resemble hyperalgesic priming. Perhaps more importantly, we also showed that targeting GRK2/EPAC1 inhibited CFA-induced hyperalgesia, a model of persistent inflammatory pain. On the basis of these results, we propose that patients with chronic pain associated with chronic inflammation (e.g., arthritic pain) could benefit from therapies targeting GRK2/EPAC1. This may be especially relevant for patients that continue to experience pain after apparently successful reduction of joint inflammation in response to treatment (63, 64). Preclinical studies should be performed to further examine these possibilities.

Local application of HSV is regarded as an ideal platform for novel therapies of chronic pain because HSV has a natural ability to infect the sensory nerve via peripheral inoculation. With a single inoculation, the virus may provide long-term therapy in restricted appropriate regions of the body (65, 66). Recently, results from a phase I clinical trial using a similar replication-deficient HSV amplicon to overexpress preproenkephalin reported no adverse effects in patients (67). Notably, a recent study in rats indicates that HSV amplicons can also be used for the targeted delivery of asODNs (68), and thus would provide a tool to locally reduce EPAC1 expression as well. These and our present findings clearly indicate that it may ultimately be feasible to use a similar approach in humans to deliver GRK2 by local administration of HSV-*GRK2* or *EPAC1* antisense DNA in humans to prevent and treat chronic pain.

Methods

Animals. Female C57BL/6 mice as well as *Epac1*$^{+/-}$ (36) and littermate WT mice aged 12–14 weeks were used. All experiments were performed in a blinded setup.

Mechanical hyperalgesia. Before experiments, mice were exposed to the equipment without any nociceptive stimulation for 1–2 h/d for 2 days. On day 3, mice were placed in the test environment 15–20 minutes before testing. Baseline responses were determined on 3 different days using von Frey hairs, and the 50% paw withdrawal threshold was calculated using the up-and-down method (25, 69). In brief, animals were placed on a wire grid bottom through which the von Frey hairs were applied (bending force range, 0.02–1.4 g, starting with 0.16 g; Stoelting). The hair force was increased or decreased according to the response. Clear paw withdrawal, shaking, or licking were considered as nociceptive-like responses. Ambulation was considered an ambiguous response, and the stimulus was repeated in such cases.

Hyperalgesic priming and CFA models. To induce hyperalgesic priming, 5 μl carrageenan (1% in saline; Sigma-Aldrich) or 5 μl ΨεRACK (1 μg in saline; obtained from the W.M. Keck Facility of Yale University) (15) was intraplantarly injected into the hind paw. Control mice received 5 μl saline.

3–14 days later, mice received an intraplantar injection of 2.5 μl PGE_2 (40 μg/ml; Sigma-Aldrich), epinephrine (4 μg/ml; Sigma-Aldrich), 8-pCPT (5.04 μg/ml; Biolog LifeScience Institute), or 5 μl recombinant mouse IL-1β (200 ng/ml; R&D Systems) per paw. For the CFA model, 20 μl CFA (Sigma-Aldrich) was injected intraplantarly.

Immunohistochemical staining of GRK2. Mice were deeply anesthetized with sodium pentobarbital (50 mg/kg i.p.) and transcardially perfused with PBS followed by 4% paraformaldehyde, after which DRG (lumbar [L3–L5] and

thoracic [T6–T10]) and sciatic nerves were collected. Tissues were post-fixed, cryoprotected in sucrose, embedded in OCT compound, and frozen at –80°C. Frozen sections of DRG and sciatic nerve (10 μm) were stained with biotinylated IB4 (10 μg/ml; Vector Laboratories) and rabbit anti-GRK2 (1:100; Santa Cruz Biotechnology). Primary anti-GRK2 antibody blocked with a GRK2 blocking peptide (Santa Cruz Biotechnology) was used as a control. Staining was visualized with Alexa Fluor 488–conjugated streptavidin (1:200; Invitrogen) and Alexa Fluor 594–conjugated goat anti-rabbit antibody (1:200; Invitrogen) and photographed with an EVOS fl (AMG Life Technologies) using identical exposure times for all slides. GRK2 levels in $IB4^+$ and $IB4^-$ small-diameter DRG neurons (<23 μm diameter; ref. 70) and in sciatic nerve fibers were analyzed with NIH ImageJ.

The average background fluorescence for specific subsets of DRG neurons or sciatic nerves (primary GRK2 antibody plus GRK2 blocking peptide) were subtracted before calculation of the percent change in GRK2 staining. Stainings were done in parallel for samples from carrageenan-, ΨεRACK-, or CFA-treated mice and their respective saline-treated controls.

Western blotting. Lumbar and thoracic DRG were frozen in liquid nitrogen and homogenized in ice-cold 50 mM Tris-HCl (pH 8), 5 mM EDTA, 150 mM NaCl, 1% NP-40, 0.5% deoxycholic acid, 0.1% SDS containing protease inhibitor mix (Sigma-Aldrich), 100 mM PMSF, 10 mM β-glycerolphosphate, 1 mM $NaVO_3$, and 20 mM NaF.

Proteins were separated by 7.5% SDS-PAGE and transferred to polyvinylidene difluoride membranes (Millipore). Blots were stained with mouse anti-EPAC1 (Cell Signaling Technology), mouse anti-EPAC2 (Cell Signaling Technology), and goat anti-actin (Santa Cruz Biotechnology) followed by peroxidase-conjugated goat anti-mouse IgG plus IgM (heavy and light chain) (Jackson Immunoresearch) or peroxidase-conjugated donkey anti-goat IgG (Santa Cruz Biotechnology) and developed by enhanced chemiluminescence (GE Healthcare). Band density was determined using a GS-700 Imaging Densitometer (Bio-Rad).

HSV-mediated GRK2 and GFP gene expression. We generated a bicistronic HSV construct into which we cloned bovine *GRK2* or $GRK2^{K220R}$ under control of the α4 promotor and in which *GFP* expression is driven by the α22 promoter (34). Both are immediate early gene promoters and have similar kinetics of expression, so the reporter can reliably be used as an indicator of transgene expression (71, 72). Control HSV-*GFP* contains *GFP* under control of the α22 promoter only. Mice were inoculated intraplantarly twice with 2.5 μl of 1.4×10^7 pfu/ml. To control for *GRK2* and/or *GFP* expression, the unfixed skin of hind paws was isolated and frozen at day 3 after the last inoculation. In addition, fixed DRG and sciatic nerve tissues were prepared as described above.

Frozen sections of skin (14 μm) were fixed in acetone and stained with rabbit anti-GFP (1:100; GeneTex) for 60 hours and overnight at 4°C. Frozen sections of skin, DRG and sciatic nerve (10 μm) were incubated with rabbit anti-GFP (1:100; GeneTex) for 60 hours. Skin was stained with mouse anti-peripherin (1:100; Sigma-Aldrich); DRG and sciatic nerve was stained with IB4 (10 μg/ml; Vector Laboratories). We used Alexa Fluor 594–conjugated streptavidin (Invitrogen) and Alexa Fluor 488–conjugated donkey anti-rabbit antibody (Invitrogen) in the second step.

Epac1 and mismatch asODNs. The *Epac1* asODN sequence (5′-AACTCTC-CACCCTCTCCCA-3′) is directed against a unique sequence of mouse *Epac1* mRNA; mismatch asODN (5′-ACATTCCACCCTCCTCCAC-3′) was used as a control. 10 μg *Epac1* asODNs or mismatch asODNs in 5 μl saline were injected intrathecally between the fifth and sixth lumbar vertebrate under isoflurane anesthesia.

In situ hybridization. In situ hybridization for *Epac1* mRNA was performed on paraformaldehyde-fixed, paraffin-embedded tissue sections (4 μm). Sections were digested with 2 μg/ml proteinase K (Exiqon) for 5 minutes at room temperature and loaded onto Ventana Discovery Ultra for in situ hybridization analysis. Slides were incubated with double digoxigenin–labeled mercury LNA RNA probe specific for *Epac1* (5DigN/TGGAGCGGTATGAGTGTGAGT/3DigN; Exiqon) for 2 hours at 50°C. Slides were developed using a polyclonal anti-digoxegenin antibody and alkaline phosphatase–conjugated secondary antibody (Ventana) with NBT-BCIP as the substrate. A double digoxigenin–labeled probe specific for U6 small nuclear RNA (Exiqon) was used as positive control, and a double digoxigenin–labeled negative control probe (catalog no. 99004-15; Exiqon) was used as a negative control.

Statistics. Data are expressed as mean ± SEM. Statistical analysis was carried out using 2-tailed Student's *t* test or 2-way ANOVA followed by Bonferroni analysis. A *P* value less than 0.05 was considered significant.

Study approval. Mice were maintained in the animal facility of the University of Utrecht. All experiments were performed in accordance with international guidelines and approved by the University Medical Center Utrecht experimental animal committee.

Acknowledgments

The authors are indebted to Robert Sapolsky (Stanford University and Stanford University School of Medicine, Stanford, California, USA) for contributing to preparation of the HSV construct and scientific editor Jeanie F. Woodruff for expert editorial assistance. Research reported here was supported by the National Institute of Neurological Diseases and Stroke, NIH (award nos. RO1NS073939 and RO1NS074999). The content is solely the responsibility of the authors and does not necessarily represent the official views of the NIH. This research was also supported by a STARS grant of the University of Texas System to A. Kavelaars.

Received for publication May 13, 2013, and accepted in revised form September 12, 2013.

Address correspondence to: Annemieke Kavelaars, Neuroimmunology of Cancer Related Symptoms (NICRS) Laboratory, Department of Symptom Research, University of Texas M.D. Anderson Cancer Center, 1515 Holcombe Boulevard, Unit 1450, Houston, Texas 77030, USA. Phone: 713.794.5297; Fax: 713.743.3475; E-mail: akavelaars@mdanderson.org.

1. National Research Council. *Relieving Pain in America: A Blueprint for Transforming Prevention, Care, Education, and Research.* Washington, DC, USA: The National Academies Press; 2011.
2. Stein C, et al. Peripheral mechanisms of pain and analgesia. *Brain Res Rev.* 2009;60(1):90–113.
3. Gold MS, Gebhart GF. Nociceptor sensitization in pain pathogenesis. *Nat Med.* 2010;16(11):1248–1257.
4. Basbaum AI, Bautista DM, Scherrer G, Julius D. Cellular and molecular mechanisms of pain. *Cell.* 2009;139(2):267–284.
5. Woolf CJ. What is this thing called pain? *J Clin Invest.* 2010;120(11):3742–3744.
6. Latremoliere A, Woolf CJ. Central sensitization: a generator of pain hypersensitivity by central neural plasticity. *J Pain.* 2009;10(9):895–926.
7. Marchand F, Perretti M, McMahon SB. Role of the immune system in chronic pain. *Nat Rev Neurosci.* 2005;6(7):521–532.
8. Wallace MS, Irving G, Cowles VE. Gabapentin extended-release tablets for the treatment of patients with postherpetic neuralgia: a randomized, double-blind, placebo-controlled, multicentre study. *Clin Drug Investig.* 2010;30(11):765–776.
9. Aasvang E, Kehlet H. Chronic postoperative pain: the case of inguinal herniorrhaphy. *Br J Anaesth.* 2005;95(1):69–76.
10. Asiedu MN, et al. Spinal protein kinase M zeta underlies the maintenance mechanism of persistent nociceptive sensitization. *J Neurosci.* 2011; 31(18):6646–6653.
11. Melemedjian OK, et al. IL-6- and NGF-induced rapid control of protein synthesis and nociceptive plasticity via convergent signaling to the eIF4F complex. *J Neurosci.* 2010;30(45):15113–15123.
12. Geranton SM, et al. A rapamycin-sensitive signaling pathway is essential for the full expression of persistent pain states. *J Neurosci.* 2009;29(47):15017–15027.
13. Jimenez-Diaz L, et al. Local translation in primary